Effects of spatial structure on stock assessment estimates of biomass and productivity for Yelloweye rockfish (*Sebastes ruberrimus*) in British Columbia

by

Midoli Bresch

B.Sc., University of Northern British Columbia, 2014

Project Submitted in Partial Fulfillment of the
Requirements for the Degree of
Master of Resource Management

in the
School of Resource and Environmental Management
Faculty of the Environment

Report No. 728

SIMON FRASER UNIVERSITY
Summer 2019

Approval

Name:	**Midoli Bresch**
Degree:	**Master of Resource Management**
Report No.:	**728**
Title:	**Effects of spatial structure on stock assessment estimates of biomass and productivity for Yelloweye rockfish (*Sebastes ruberrimus*) in British Columbia**
Examining Committee:	**Chair:** Meghan Burton Master of Resource Management Candidate

Sean Cox
Senior Supervisor
Professor

Kendra Holt
Supervisor
Biologist Level III
Fisheries and Oceans Canada

Date Defended/Approved: June 24th, 2019

Abstract

Ignoring the underlying structure of populations can lead to sub-optimal management of fisheries resources. I examined the influence of spatial population structure assumptions on stock assessment estimates of biomass and productivity for Yelloweye rockfish in British Columbia, Canada. Delay-difference assessment models were fit to different scenarios in which discrete stocks were delineated at successively smaller spatial scales. My results show that, in some scenarios, uncertainty in stock assessment outputs was no greater at finer spatial scales than for the aggregate stock. There was also evidence of differences in stock status at finer scales, suggesting that it might be worthwhile to establish methods for tracking Yelloweye on a finer spatial scale. Comparisons between the aggregated, coast-wide stock, and disaggregated north and south assessments would allow tracking of any differences in responses to management, providing additional certainty regarding management options and potentially lead to improved outcomes for the species.

Keywords: Yelloweye Rockfish; Delay-difference assessment models; Spatial models; British Columbia

Acknowledgements

I would like to thank the MITACS organization, Wild Canadian Sablefish, the Pacific Halibut Management Association, and the Canadian Groundfish Research and Conservation Society for their generous financial contribution to this research.

Thank you to my senior supervisor, Dr. Sean Cox, for teaching me so much and always being generous with your knowledge. Thank you to my second supervisor, Kendra Holt, for the thoughtful and timely feedback. I am very grateful to both of you.

I am beyond grateful to the PhD students in the Quantitative Fisheries Lab, Sam, Vania, Michelle, and Steve for all their patience and mentoring. I am especially grateful to Sam Johnson. Without your help and encouragement over the past three years I wouldn't have finished my Master's, and that's the truth. Thank you also to Beau, for so much assistance with sorting out the data and making it useable.

A huge thanks to my entire REM family, with whom it was a joy to live, work, and play alongside for the past three years. Thank you to my dear phat phish phriends in the Q-fish lab, Claire, Angus, and Jessica. I'm so lucky I had all of you here with me.

Thanks to Sue, Iris, Elissa, and Laurence in REM. You really are the very best support team a student could ask for and your hard work does not go unnoticed!

Finally, and as always, I would like to thank my family for this extraordinary life.

Table of Contents

Approval ii
Abstract iii
Acknowledgements iv
Table of Contents v
List of Tables vii
List of Figures viii
List of Acronyms x

Introduction 1
Study Area and Species 2

Methods 5
Description of Scenarios 5
Data 6
  Commercial Catch 6
  Recreational and Indigenous Harvest 7
  Research Surveys 7
  Biological Data 9
Delay-difference Assessment Model 9
  Growth and Age at Recruitment Analyses 9
  Natural Mortality 11
  Stock-Recruitment Relationships 11
  Population Dynamics 13
  Stock Status Indicators and Reference Points 14
Parameter Estimation 15
  Penalized Log-Likelihoods 17
Sensitivity Analyses 17
  Survey Indices 17
  Natural Mortality 18
  Penalty on Steepness 18
  Penalty on Initial Biomass 18
  Age at Knife-edge Recruitment 18
  Stock-Recruit Relationship 19

Results 21
Biological Data 21
Trends in Abundance Indices 21
Parametric Versus Non-parametric Bootstraps 23
Reference Case Results 24
Sensitivity Analyses 33
  Survey Indices 34

Penalty on Steepness 35
Exponential Penalty on Initial Biomass 37
Natural Mortality 38
Age at Recruitment..... 38
Stock Recruitment Relationship 41

Discussion..... 43

References..... 50

Appendix A: Growth Analyses 55

Appendix B: Results of Sensitivity Analyses..... 58

Appendix C: Average Recruitment Relationship Results 66

List of Tables

Table 1. Parameters derived from biological samples of Yelloweye collected from hook and line surveys. Observations equals the number of biological samples used to derive growth parameters for each stock, *k* is the estimated age at knife-edge recruitment, is the intercept and is the slope of the Ford-Walford plot. These values were used to parameterize the reference models for each stock. 11

Table 2. Fixed input parameter values for natural mortality, *M*, and specifications for penalized log-likelihoods on steepness and initial biomass used for sensitivity analyses in the delay-difference models..... 18

Table 3. Range of ages (years) tested in sensitivity analyses on the knife-edge recruitment parameter, *k.* Table headings correspond to the names of the sensitivity runs and are consistent throughout the document. 19

Table 4. Maximum likelihood estimates for catchability *q,* and survey standard deviation, *sd*, for IPHC, PHMA North and PHMA South long line surveys for each stock. 23

Table 5. Successful bootstrap iterations relative to total attempted iterations for the reference case model runs for each Yelloweye stock. Unsuccessful iterations were those for which *optim* did not achieve convergence, or where catch exceeded estimated biomass in any year of the time series. 25

Table 6. Median parameter estimates, reference points, and derived quantities from the reference runs. 5^{th} and 95^{th} percentiles are shown in parentheses. All biomass values are in tonnes. 31

List of Figures

Figure 1. Maps of four spatial scenarios where each panel represents a different hypothesis about the underlying spatial structure of outside Yelloweye in British Columbia. Labels in each panel correspond to the 12 discrete stocks assessed and are used to refer to each stock throughout this document. Shapefiles were provided by Fisheries and Oceans Canada.. 6

Figure 2. Relative abundance time series for the IPHC, PHMA North and PHMA South long line surveys by stock area. 22

Figure 3. Frequency distributions and median estimates for the steepness parameter *h.* Both parametric and non-parametric bootstrap results are shown for comparison between the two methods. 24

Figure 4. Parametric bootstrapped distributions and penalized log-likelihoods for the steepness parameter *h* for 12 Yelloweye stocks. Vertical lines show the mean of the distribution for the penalized log-likelihood, which was the same for all stocks, and the median estimate from the bootstrap procedure. The shaded area covers the standard deviation around the mean of the penalized log-likelihood. Note that the scale of the y-axis is different for each panel. 26

Figure 5. Parametric bootstrapped frequency distributions, and median B_0 estimates for each Yelloweye stock. Jeffrey's penalty on B_0 was uninformative over the range of the bootstrap distribution for all stocks. 27

Figure 6. Estimated biomass time series for each Yelloweye stock. Both the MLE and median bootstrap estimated time series are plotted. Catch is shown as vertical bars on the x-axis, and annual survey CPUEs are plotted as points. 50%, 75%, 90% and 95% bootstrapped confidence intervals are shown as polygons in ascending shades of grey. The time series are truncated, as there was relatively little change in biomass prior to the mid-80s. 28

Figure 7. Median estimated harvest rate over time for each Yelloweye stock. Shaded areas represent the 95% bootstrapped confidence interval. The red horizontal line is the median estimate for U_{MSY}. 30

Figure 8. Estimated stock status in 2017. Yelloweye stocks are arranged generally in order of spatial scenarios i.e. the first scenario, the coast-wide stock is plotted first. Horizontal lines indicate 95% bootstrapped confidence intervals and dashed vertical lines demarcate the critical, cautious, and healthy status zones. 32

Figure 9. Median estimated biomass time series for each aggregate stock and the summed estimated biomass of its components stocks. Refer to figure 1 for the map showing spatial breakdown of aggregate stocks into component stocks. Time series have been truncated. 33

Figure 10. MLE biomass time series for each Yelloweye stock from sensitivity analyses on model fits to individual relative abundance indices. Results from the reference case, where stocks were fit to all survey indices are shown for comparison. 35

Figure 11. Frequency distributions for bootstrapped estimates of the steepness parameter *h* with a mean of 0.67 and low (0.11), reference (0.17), and high (0.21) values for standard deviation of the penalized log-likelihood. Vertical lines show the median steepness estimate for each of the low, reference, and high scenarios. 37

Figure 12. Changes to stock status in 2017 as a result of sensitivity analyses on the penalty for steepness (low_*h* and high_*h*), fixed natural mortality rate (low_*M* and high_*M*), and age at knife-edge recruitment (low_*k* and high_*k*). Yelloweye stocks are arranged generally in order of spatial scenarios i.e. the first scenario, the coast-wide stock is plotted first. Reference case results are shown in the top panel for comparison. Input parameters for the sensitivity analyses are reported in table 2. 5^{th} and 95^{th} percentiles are shown as horizontal bars. 39

Figure 13. Changes to stock status in 2017 as a result of sensitivity analyses on age at knife-edge recruitment, *k,* for each Yelloweye stock. All other input parameters were kept the same as for reference case runs. Yelloweye stocks are arranged generally in order of spatial scenarios i.e. the first scenario, the coast-wide stock is plotted first. The 5^{th} and 95^{th} percentiles are shown as horizontal bars. Reference case results are shown in the top panel for comparison. 41

List of Acronyms

BC	British Columbia
DFO	Fisheries and Oceans Canada
IFMP	Integrated Fishery Management Plan
IPHC	International Pacific Halibut Commission
ITQ	Individual Transferrable Quota
MLE	Maximum Likelihood Estimate
PGMA	Pacific Groundfish Management Area
PHMA	Pacific Halibut Management Association
RCA	Rockfish Conservation Area
RCS	Rockfish Conservation Strategy
SARA	Species At Risk Act
SRR	Stock Recruitment Relationship
TAC	Total Allowable Catch

Introduction

In fisheries, single-species units, or stocks, determine the scale at which the effects of fishing are monitored and on which management decisions are applied. Stock boundaries may be delineated based on genetic analysis, unique demographics, habitat features, historical fishing patterns, or a combination of these factors (Stephenson, 1999). In the absence of empirical evidence for heterogeneous spatial structure, stock boundaries can also be assigned based on political and administrative boundaries (Berger et al., 2017). Determining the true underlying spatial structure of a population can be challenging (Ciannelli et al., 2008), and the data and resources necessary for this work are often limited or unavailable (ICES, 2011). It is generally simpler for fisheries managers to assume a homogenous stock structure, and manage accordingly by aggregating data and allocating harvest for a single fleet (Cope and Punt, 2011). This style of management persists, despite widespread acceptance amongst fisheries scientists that most stocks exhibit some degree of spatial population structure (Berger et al. 2017, Ciannelli et al., 2008).

Ignoring the underlying structure of populations can lead to sub-optimal management of fisheries resources (Berkeley et al., 2004; Guan et al., 2013). For example, if sub-populations exist, fishing as if they are a single large population can disproportionately exploit less productive units, potentially resulting in localized depletion or extirpation of individual sub-populations (Berger et al. 2017; Hilborn and Walters, 1992). Loss of sub-populations could have negative implications for the long-term resiliency and adaptability of species (Hilborn et al., 2003). Conversely, ignoring spatial structure could result in overestimating exploitation rates in some areas, leading to economic losses from foregone yield (Booth, 2000). Given potential biological and economic consequences of ignoring spatial structure, contemporary management could benefit from allocating resources toward improving our understanding of underlying structural complexity of exploited stocks (Stephenson, 1999; Cadrin and Secor, 2009).

Simulation experiments are typically used to study the interactions between spatial population structure, the scale of stock assessments, and the allocation of fishing pressure (Cope and Punt 2011; Punt, 2019; Jardim et al., 2018). Simulation allows the researcher to identify and evaluate various trade-offs that arise when contemplating

management on a spatial scale. For example, assessing stocks at smaller spatial scales involves partitioning the available data, sacrificing the quantity of information available to each sub-assessment and potentially increasing uncertainty in the outputs (Chen et al., 2003). Data scarcity means that spatially disaggregated stock assessments don't automatically translate to better performance over aggregate assessments (Guan et al., 2013). However, if the scale of the assessment matches the true population structure, better management advice could be achieved, despite the reduction in data for each assessment area (Cope and Punt, 2011). Exploring the implications of spatial complexity though simulation-estimation experiments is increasingly common (Goethel and Berger, 2017; Guan et al., 2013; Kerr et al., 2014), but incorporating spatial structure within stock assessments aimed at providing management advice remains challenging and less common (Punt, 2019). In this paper, I investigate the effects of alternative hypotheses about spatial population structure on assessment outcomes for Yelloweye rockfish in British Columbia (B.C.), Canada.

Study Area and Species

Yelloweye rockfish, (*Sebastes ruberrimus),* are a long-lived, slow-growing species with late age-at-maturity (Love et al., 2002). Adult Yelloweye are habitat specialists, preferring demersal, rocky habitats, which have a discontinuous, patchy distribution on the B.C. coast (Yamanaka et al., 2006). They are sedentary as adults but planktonic larvae are likely dispersed by ocean currents, although the dispersal pattern and extent are unknown (Yamanaka et al., 2000). Yelloweye in B.C. are divided into two discrete management units, delineated based on the results of two coast-wide genetic analyses (Yamanaka et al., 2000; Siegle et al., 2013). The inside population inhabits the waters between Vancouver Island and the mainland, including the Strait of Juan de Fuca (area in black in figure 1). The outside Yelloweye stock inhabits the rest of the B.C. coast, including Haida Gwaii and the west coast of Vancouver Island (Yamanaka et al. 2000). My research focuses on the outside Yelloweye population, which, hereafter, I refer to simply as Yelloweye.

Fisheries and Oceans Canada (DFO) manages Yelloweye under an Integrated Fisheries Management Plan (IFMP) for west coast groundfish species. The groundfish IFMP applies to seven different fishery sectors and allocates catch based on individual transferable quotas (ITQs). A large portion of the Total Allowable Catch (TAC) for

Yelloweye is caught during annual fishery independent surveys to support ground fish management. Yelloweye harvest occurs in the Halibut and rockfish hook and line fisheries and they are a popular target for recreational anglers. There is some by-catch mortality in groundfish trawl and Salmon troll fisheries. Recreational fisheries are managed by daily bag limits, and catch is monitored through a combination of creel surveys, lodge and guide logbooks, and e-mail angler surveys (DFO, 2017).

Beginning in 2002, DFO implemented a series of conservation measures aimed at reducing fishing mortality rates on Yelloweye. Under the Rockfish Conservation Strategy (RCS), 20% of available habitat on the outer coast was designated as rockfish conservation areas (RCAs) and closed to all commercial and recreational fishing, although illegal fishing continues in some RCAs (Haggarty et al., 2016). Since 2006, all commercial groundfish fisheries have been subject to 100% catch monitoring (Yamanaka and Logan, 2010) and full retention of by-catch species (DFO, 2017). Yelloweye were listed as a Species of Special Concern, under the federal Species At Risk Act (SARA), in 2011 (SARA Public Registry).

The most recent stock assessment for outside Yelloweye showed no evidence that the management measures implemented under the RCS are resulting in recovery of Yelloweye (Yamanaka et al., 2018), which is not surprising, given the long generation time of Yelloweye. DFO's current management objective is to maintain or increase Yelloweye distribution and abundance (DFO, 2018) through stepwise reductions in overall TAC to 100 tonnes by 2019 (DFO, 2017). A low TAC for Yelloweye could impact other fisheries managed under the groundfish IFMP. For example, Yelloweye are captured incidentally in the fishery for Pacific Halibut (*Hippoglossus stenolepsis)*, which is an abundant, high-value species (DFO, 2017). Harvesting the full quota of Yelloweye as bycatch in the Halibut fishery would result in closure of the entire outside commercial groundfish fishery, resulting in very large losses of harvest value and employment. An increase in Yelloweye yield would benefit the rest of the groundfish industry by providing flexibility to fully utilize TACs for more productive and valuable species. Thus, there are economic as well as conservation objectives that would benefit from improving stock assessment advice for Yelloweye.

Two separate genetic studies failed to find evidence of spatial population complexity for outside Yelloweye, although both studies caution that the lack of evidence

should not be interpreted as confirmation that such complexity does not exist, because the gene flow required to maintain genetic homogenization in marine fishes is very low (Yamanaka et al., 2000; Siegle et al., 2013). Yelloweye life history characteristics, such as site fidelity, late age-at-maturity, and long life expectancy increase the likelihood that spatially heterogeneous fishing effort could have imposed some form of stock structure, even if, in its unexploited state, spatial structure was homogenous (Berkeley et al., 2004; Cope and Punt 2011). Fishing-induced changes to local abundance or productivity are likely to go undetected under aggregate stock management (Goethel and Berger, 2017), which could be problematic for Yelloweye, because depleted populations are not likely to be replenished from more abundant populations within a reasonable timeframe (Yamanaka et al., 2000). It follows that the management implications of discrete stock structure should be explored for Yelloweye in B.C.

In this paper, I examine the influence of spatial population structure assumptions on stock assessment estimates of biomass and productivity for Yelloweye. Specifically, I examine four different scenarios in which discrete stocks were delineated at successively smaller spatial scales. I then fit delay-difference assessment models to data for these hypothesized Yelloweye “stocks” (Deriso, 1980; Schnute, 1985), and compare results among spatial scale scenarios. My objective was not to establish new management units for Yelloweye, or update the previous stock assessment, but rather, to use the available data for Yelloweye to assess the relative difference in stock status under specific assumptions about stock structure. Increasing our understanding of the differences and similarities between stock assessment outputs at various spatial scales may help inform future decisions about the appropriate spatial scale for stock assessments, harvest advice, and recovery planning for Yelloweye in B.C.

Methods

Description of Scenarios

The range occupied by the outside population of Yelloweye rockfish consists of the combined areas of Pacific Groundfish Management Areas (PGMAs) 3C, 3D, 5A, 5B, 5C, 5D, and 5E (figure 1, panel 4), which encompasses all marine territorial waters in B.C., excluding the region between Vancouver Island and the mainland. My analysis consisted of four scenarios, in which Yelloweye catch, survey data, and biological data were aggregated at successively smaller spatial scales. The first scenario mimicked the recent DFO assessment by lumping all outside Yelloweye data into a single coast-wide assessment (figure 1, panel 1). In scenario two, the data were divided into discrete northern (PGMAs 5E, 5D, and 5C) and southern (PGMAs 5B, 5A, 3D, and 3C) stock units. The boundary between northern and southern stocks was chosen to align with two Pacific Halibut Management Association (PHMA) longline surveys that sample the north and south coast in alternating years. In the third scenario, data were split into four discrete stocks by further isolating a single PGMA from each of the northern (isolated Area 5E) and southern (isolated Area 3C) stocks. In the fourth scenario, the spatial delineation for the stocks was matched to the PGMAs (figure 1, panel 4). Overall these scenarios resulted in 12 discrete Yelloweye stocks on which assessments were performed.

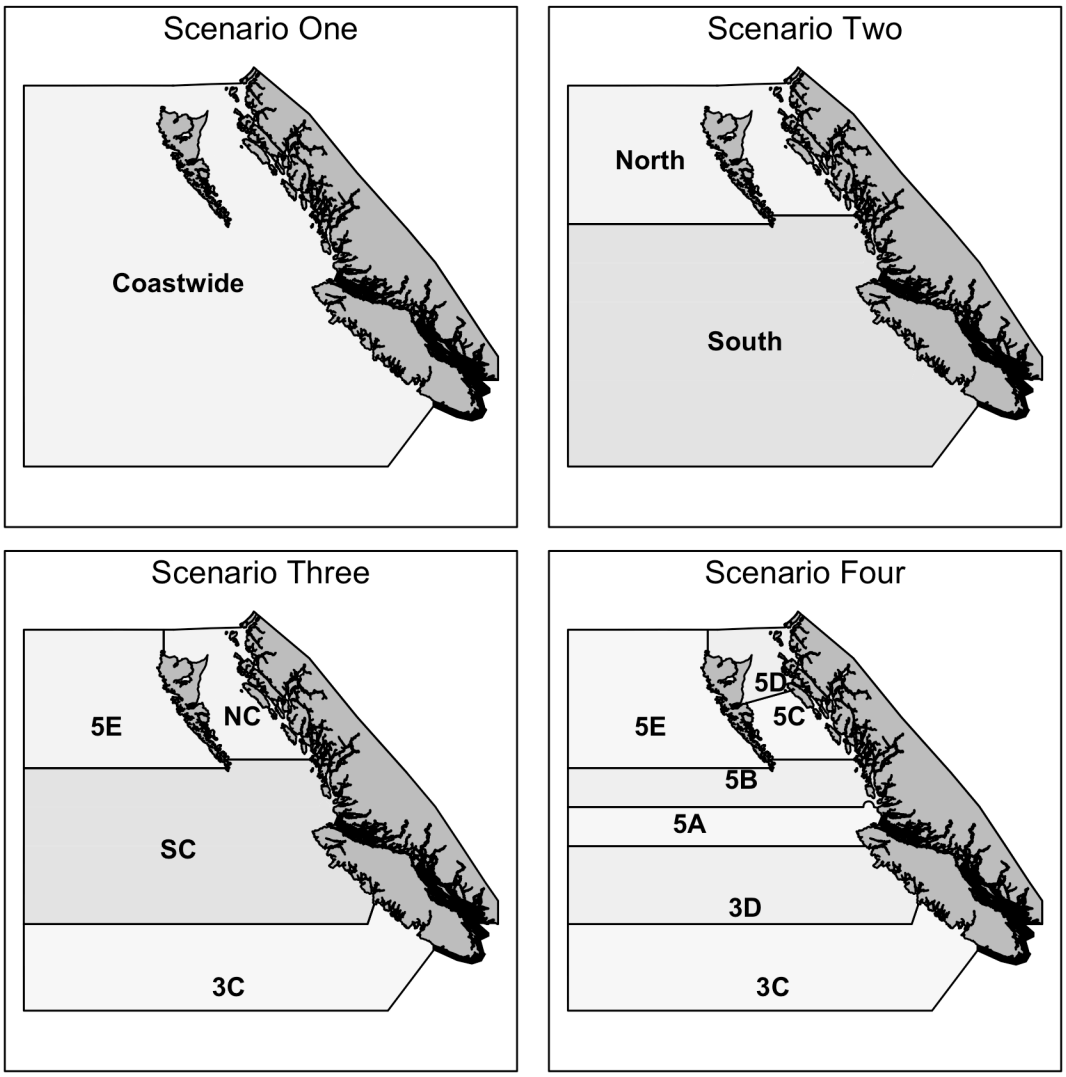

Figure 1. Maps of four spatial scenarios where each panel represents a different hypothesis about the underlying spatial structure of outside Yelloweye in British Columbia. Labels in each panel correspond to the 12 discrete stocks assessed and are used to refer to each stock throughout this document. Shapefiles were provided by Fisheries and Oceans Canada.

Data

Commercial Catch

A time series of reconstructed commercial catch from 1918 to 2017 was obtained from DFO (pers comm, Maria Surry). Data was provided for all west coast trawl and line fisheries, the Pacific Salmon troll fishery, the Dungeness crab, and the Spot Prawn

fisheries. Catch data from 2007 onward is considered fully reported, but prior to that the data were reconstructed from a combination of fisher logbooks, sales slip data, at-sea observer logbooks, and dockside monitoring programs using methods reported in Yamanaka et al. (2018).

Recreational and Indigenous Harvest

I did not include recreational or indigenous Yelloweye harvest in my analyses. Recreational catch data were available, for some areas of the coast, for the years 1984 to 2017 but, from 1984-2000, rockfish were not identified to species. Thus, summing the available data for recreational fisheries does not provide a coast-wide estimate of Yelloweye catch. A coast-wide catch reconstruction for recreational catch up to 2014 was developed for the last DFO assessment (Yamanaka et al. 2018). However, this time-series was not available for my analysis. In addition the data likely could not be reliably disaggregated to my smaller spatial scenarios. Resolving these issues with the recreational catch was beyond the scope of this project. For similar reasons I did not include indigenous food, social, and ceremonial catch.

Data from the most recent DFO assessment of Yelloweye show that, from about 1950 to the early 1980s recreational catch accounted for greater than 50% of total Yelloweye catch, on a coast-wide scale. Later, recreational catch declined as a percentage of total removals and commercial catch dominated the peak catches during the 1980s and early 90s (Yamanaka et al., 2018). Excluding recreational and indigenous catch from my analysis biased my estimates for biomass; therefore, my results should not be interpreted as an update to the last assessment in 2014.

Research Surveys

Data for three fishery independent survey indices were provided by DFO (pers comm, Maria Surry). The International Pacific Halibut Commission (IPHC) has operated an annual, fixed station, longline survey on a 10 nautical mile grid along the west coast since 1963. Beginning in 1998, 20% of hooks fished were sampled for species other than Halibut, so catch per unit effort (CPUE) was scaled by the number of hooks observed for this time period. Since 2003, all rockfish caught in the survey have been enumerated by species, and some biological data has been collected (Yamanaka et al., 2018). The IPHC survey is designed to index Pacific Halibut, which have different habitat

preferences than Yelloweye rockfish. Some survey locations occur outside typical Yelloweye habitat, so I removed all stations that had never caught Yelloweye in any year of the time series.

The PHMA hard bottom long line survey, operating annually since 2006, is a coast-wide, depth-stratified survey, designed to index rockfish species in British Columbia. The survey alternates between the north and south coast, so that each PGMA is sampled every other year. North and South PHMA time series were therefore treated as separate indices throughout my analysis. PHMA CPUE estimates were stratified by depth and area using standard Cochran estimators (Cochran, 1977), allowing me to calculate a relative index proportional to the area sampled in each stratum. Latitude and longitude for each fishing event in each survey allowed me to place each event within its corresponding PGMA.

A portion of Area 5B, on the southern tip of Haida Gwaii, is surveyed in both the PHMA North and PHMA South survey years. The rest of Area 5B is surveyed in the South. Data from the portion of 5B surveyed by the PHMA North were left in the north and added to CPUE calculations for Area 5E (west coast of Haida Gwaii). The PHMA South sampling events in this area were removed from CPUE calculations for the rest of Area 5B in all scenarios. IPHC fishing events that overlapped with this section of 5B were also removed from CPUE calculations for 5B and added to CPUE calculations for Area 5E and the northern scenarios. I was unable to split commercial catch from Area 5B in the same way, as it is not Georeferenced at that fine a resolution. Therefore, all commercial catch for 5B was left in Area 5B.

IPHC, PHMA North, and PHMA South surveys were treated as indices of relative abundance. I assumed each index $I_{i,t}$ was proportional to biomass in a given year, *t,* i.e.,

$$I_{i,t} = q_i B_t \tag{1}$$

where the parameter q, or catchability coefficient, was estimated in the model and used to scale the model biomass B_t to the expected value of observed indices (Hilborn and Walters, 1992).

Biological Data

Georeferenced length and age data from IPHC and PHMA longline surveys, as well as the Yelloweye Rockfish Charter Longline Survey, and the Combined Submersible and Fishing Survey were provided by DFO (pers comm, Maria Surry) for the years 1997-98, 2000, 2002-12, and 2014-15. Age and length data were used in growth analyses to estimate parameters which are inputs to the delay-difference stock assessment model, described below. Length data from trawl surveys was excluded from growth analyses because they lacked associated age data.

Delay-difference Assessment Model

Yelloweye are a long-lived species, with a relatively late age-at-50%-maturity (Yamanaka et al. 2018), and delay-difference models explicitly account for such a lag in recruitment (Deriso, 1980; Schnute, 1985). Delay-difference models aggregate abundance in just two stages (adult and recruit) but they allow the modeller to incorporate ancillary information on growth, natural mortality, and age-at-maturity without the extensive data requirements of fully age-structured models (Meyer and Millar 1999; Hilborn and Walters, 1992).

Growth and Age at Recruitment Analyses

Delay-difference models rely on several assumptions about growth and recruitment. The first assumption is that weight at age w_a is described by the Brody growth equation

$$w_a = \alpha + \rho w_{a-1} \tag{2}$$

Where α and ρ are the intercept and slope of the Ford-Walford plot of weight-at-age *a* versus weight-at-age *a + 1* (Ricker, 1975). The second key assumption of the delay-difference model is so called “knife-edge” recruitment, which occurs at age=*k;* that is, fish aged *k* or greater are sexually mature and equally vulnerable to the fishery (Hilborn and Walters, 1992). Length and age data, described above, were used to estimate stock specific von-Bertalanffy growth parameters (Appendix A, table 1) and weight-at-age tables. The von-Bertalanffy parameters were not used directly within the delay-difference models, though I did examine them for differences in growth between spatial scales.

Results from the growth analyses were used to derive specific values for α, ρ and *k,* which are inputs for the delay-difference assessment model.

To estimate *k* for each stock, I fit a spline to the estimated weight-at-age curve. The *uniroot* function in R was used to solve for the root of the spline function (the inflection age) in each weight-at-age curve (Appendix A, figure 1). Because the inflection point returned by *uniroot* is a continuous number, the R functions *floor* and *ceiling* were used to find discrete values for low and high estimates of the inflection age. The age returned by the *ceiling* function was used as the age at knife-edge recruitment *k* for the reference case stock assessments (table 1). The *floor* age estimate and modal age in each set of biological samples were used to parameterize model runs for sensitivity analyses on *k*.

In the delay-difference model unique α and ρ values must be estimated for each value of age-at-recruitment *k*, e.g. for reference case runs as well as for all sensitivity analyses on *k.* To parameterize each model run for each stock, Ford-Walford plots were created for age *k* and above and α and ρ were estimated using linear regression. Ford-Walford parameters for the reference case runs for each stock are reported in table 1.

Table 1. Parameters derived from biological samples of Yelloweye collected from hook and line surveys. Observations equals the number of biological samples used to derive growth parameters for each stock, *k* is the estimated age at knife-edge recruitment, α is the intercept and ρ is the slope of the Ford-Walford plot. These values were used to parameterize the reference models for each stock.

Stock	Observations	*k* (yrs.)	α (Tonnes)	ρ
CW	30699	14	0.000175	0.9690
N	15803	14	0.000194	0.9652
S	14866	14	0.000165	0.9702
NC	5017	14	0.000190	0.9656
SC	14279	14	0.000173	0.9692
5E	10786	14	0.000193	0.9662
5D	935	15	0.000211	0.9607
5C	4082	14	0.000185	0.9666
5B	4421	14	0.000162	0.9715
5A	5887	13	0.000158	0.9706
3D	3971	15	0.000183	0.9691
3C	587	12	0.000132	0.9767

Natural Mortality

The third, and final, key assumption of the delay-difference model is that the natural mortality rate *M* is constant over both time and age (Deriso, 1980). For my reference case models, natural mortality was fixed at 0.0386 yr^{-1}, which was the same as assumed in the last assessment DFO assessment in 2014.

Stock-Recruitment Relationships

Stock-recruitment relationships (SRRs) are used within assessment models to link adult spawning stock size to the resulting number of recruits produced (Hilborn and Walters, 1992). Stock assessment models typically allow the analyst to choose a sub-

model for recruitment that represents the assumed reality of the stock, although the most appropriate choice of SRR is often not obvious (Mangel et al., 2010). The most recent Yelloweye assessment by DFO used a Ricker SRR (Yamanaka et al., 2018), but I chose to use a Beverton-Holt SRR. In the Ricker function, recruitment is allowed to decrease when the adult spawning population is high, mimicking over compensation in density dependence (Ricker, 1954). DFO used a Ricker SRR based on evidence of spatial overlap between adult and juvenile Yelloweye habitat and potential cannibalism on juveniles; however, empirical studies show that juvenile and adult Yelloweye are spatially separated by depth (Yamanaka et al. 2006), which decreases the likelihood of cannibalism. Furthermore, a meta-analysis of 128 fish species also identified the Beverton-Holt SRR as the preferred model (Punt et al., 2005) and recent stock assessments for other *Sebastes* species in British Columbia also use a Beverton-Holt SRR (Starr and Haigh, 2017; DFO, 2012).

The Beverton-Holt (Beverton and Holt, 1957) SRR describes recruitment in year *t, R_t,* as increasing, with increasing number of spawners, to some asymptotic value and, unlike the Ricker SRR, the number of recruits does not decline at high spawner density. In the delay-difference assessment model Beverton-Holt recruitment takes the form

$$R_t = \frac{aB_{t-k}}{1+bB_{t-k}} \tag{3}$$

Where R_t is recruitment in years *t* greater than age-at-recruitment *k* and B_{t-k} is biomass in year *t* minus *k,* which incorporates the lag in recruitment into the model. The constant *a* is the slope of the SRR function at its origin, or the maximum number of recruits possible, and the constant *b* is a scaling factor representing the spawning stock in the absence of fishing (Hilborn and Walters, 1992).

In this paper, I define the Beverton-Holt constants a and b in terms of the steepness parameter h (Mangel et al., 2010).

$$a = \frac{R_0 4h}{B_0(1-h)} \tag{4}$$

$$b = \frac{5h-1}{B_0(1-h)} \tag{5}$$

Where R_0 is unfished recruitment and B_0 is unfished biomass. Steepness h is defined as the recruitment potential of the stock when the spawning biomass is at 20% of unfished biomass (Mace and Doonan, 1988). It is believed to provide an indication of a stock's ability to recover from low population sizes, and thus its resilience to harvest (Thorson et al., 2018). The steepness parameter allows for easy comparison of productivity amongst different stocks, and is commonly estimated in fisheries stock assessment (Mangel et al., 2010), even though this can be problematic, especially when the data are likely to be uninformative, or a so-called "one-way-trip" (Hilborn and Walters, 1992). However, steepness is inextricably linked to particular stocks' demographics and attempts should be made to estimate it in assessment models (Mangel et al., 2010).

Population Dynamics

The following equations (Eq. 1.6 to 1.8) describe how the modeled population is initialized at unfished equilibrium in the delay-difference models. Mean weight at equilibrium is first calculated as

$$\overline{w} = \frac{e^{-M}\alpha + w_k(1-e^{-M})}{1-\rho e^{-M}} \tag{6}$$

Initial numbers of Yelloweye are then unfished biomass divided by unfished mean weight, i.e.,

$$N_0 = \frac{B_0}{w_0} \tag{7}$$

Equilibrium recruitment is initiated as

$$R_0 = \frac{aB_0}{1+bB_0} \tag{8}$$

The delay-difference model then updates the number of fish and total biomass, respectively, via.

$$N_t = S_{t-1}N_{t-1} + R_t \tag{9}$$

$$B_t = S_{t-1}(\alpha N_{t-1} + \rho B_{t-1}) + w_k R_t \tag{10}$$

where the annual survival rate is

$$S_t = e^{-M}(1-U_t) \tag{11}$$

U_t is the exploitation rate ($U_t = \frac{C_t}{B_t}$), and R_t is recruitment in year t after age at knife-edge recruitment k.

Stock Status Indicators and Reference Points

Fisheries management targets are often defined according to the concept of maximum sustainable yield (MSY), or the long-term maximum yield that could be harvested at equilibrium (Hilborn and Walters, 1992). The MSY concept is rooted in the assumption that an exploited stock can achieve equilibrium, where removals at some harvest rate result in no net change in population size (Schaefer, n.d). Under this assumption it is possible to estimate B_{MSY} the equilibrium biomass that produces MSY and the associated fishing mortality, F_{MSY} (Hilborn and Walters, 1992). There is no direct analytical relationship between MSY and any parameter in the delay-difference model (Meyer and Millar, 1999), but these reference points can be computed numerically over a vector of potential fishing mortality F_e by applying the following equilibrium equations for each value of F_e.

For the Beverton-Holt SRR the starting conditions for survival S_e, mean weight w_e, and biomass B_e for each stock were initialized in 2018 at equilibrium, for each value of F_e (Starr and Haigh, 2017):

$$S_e = \exp^{-(M+F_e)} \tag{12}$$

$$\overline{w}_e = \frac{S_e\alpha + w_k(1-S_e)}{1-\rho S_e} \tag{13}$$

$$B_e = -\frac{(-\overline{w}_e + S_e\alpha + S_e\rho\overline{w}_e + \overline{w}_k a\overline{w}_e)}{b(-\overline{w}_e + S_e\alpha + S_e\rho\overline{w}_e)} \tag{14}$$

Equilibrium yield, Y_e, was estimated using the Baranov catch equation

$$Y_e = \frac{F_e}{(F_e + M)}(1 - \exp^{-(F_e+M)})B_e \quad (15)$$

For each stock the value of F_e that resulted in the greatest sustained yield was the estimate of F_{MSY} and the associated equilibrium biomass was the estimate of B_{MSY}. I obtained precision of 0.001 on these values by testing 400 values of F_e, ranging from 0.001 to 0.4 in increments of 0.001.

DFO's precautionary approach to fisheries management defines three status zones to denote the health of a stock based on the ratio of current biomass to B_{MSY} (DFO, 2006). The three status zones are delineated by reference points set at $0.4B_{MSY}$, the upper limit of the "critical" zone, and $0.8B_{MSY,}$ the lower limit of the "healthy" zone. Stock status between these two zones is defined as "cautious". Stock status was assessed for each Yelloweye stock and used to compare results from reference case runs and sensitivity analyses.

Parameter Estimation

All models were developed and analyzed in R version 3.5.2 (R Core Team, 2018). All stock assessment models were fit using the general-purpose optimization function *optim* to minimize an objective function combining the negative log-likelihood of the data with penalties on steepness and initial biomass, as well as penalties to ensure that model biomass remained positive (i.e. I imposed an additional penalty if catch exceeded estimated biomass in any year). Optimization for each stock was a two-step procedure, with the first step calling *optim* with initial estimates of h and B_0 using the Nelder-Mead non-derivative-based minimization algorithm (Nelder and Mead, 1965) followed by a second *optim* call using the BFGS method, which uses numerical derivatives.

Ninety-five percent confidence intervals for estimated parameters were approximated via non-parametric bootstrapping, in which I generated new pseudo-datasets by re-sampling the residuals from the best-fit model (Efron, 1979). In a non-parametric bootstrap, the distribution of the sample is assumed to be representative of

the true underlying distribution. Each observation Y_i^{obs} for *i* =1…*n* was fit using the delay-difference model, generating predicted values Y_i^{pred} for each survey index. Log-residuals were calculated by subtracting the predicted values from the observed.

$$r_i = \log Y_i^{obs} - \log Y_i^{pred} \tag{16}$$

New datasets were generated by randomly re-sampling residuals, with replacement, and adding a residual to each predicted survey index data point (Hilborn and Walters, 1992).

Parametric bootstrapping assumes the observed sample is drawn from a population that can be explained by a specified probability distribution (Efron, 1985). For the parametric bootstrap, pseudo-datasets were generated via a random residual error, e_i added to each best-fit model value. Each log-residual error term was drawn from a normal distribution with a mean, $\mu = 0$ and a standard deviation, σ equal to the estimated standard deviation for each survey from the MLE estimate.

$$e_i \sim Normal(\mu, \sigma^2) \tag{17}$$

In both parametric and non-parametric bootstrapping, the model is fit to each pseudo-dataset to obtain a new set of parameter estimates. The variance of the resulting distribution of estimates is an approximation of the true estimation variance of the parameter or derived quantity (Hilborn and Mangel, 1997).

Both parametric and non-parametric bootstraps have their limitations. Parametric bootstrapping can result in samples that are outside the range of observed data, which may not be realistic, while non-parametric methods can lead to underestimating the variance of the sampling distribution, especially if the sample size is small (Chernick and LaBundde, 2011). I used both parametric and non-parametric bootstrap methods to examine differences in results arising from these potential pitfalls. To ensure I completed an adequate number of bootstrap replicates for each stock, I simultaneously ran two bootstrap procedures, each with a different random seed value. I then plotted the coefficient of variation of the bootstrapped estimates against the number of bootstraps. When the resulting lines for each random seed value had converged and remained

visually flat I used the corresponding number of bootstraps to estimate medians and 95% confidence intervals for the various model runs.

Penalized Log-Likelihoods

I utilized a penalized-likelihood approach to estimate parameters *h, B_0* and *q* in which a penalty on *h* and B_0 parameters shifted the MLE estimates toward values grounded in information external to the likelihood (Cole et al., 2013). The penalty I used for steepness was based on a hierarchical meta-analysis of rockfish stock recruitment data (Forrest et al., 2010). I implemented this constraint on steepness via a Beta distribution (mean = 0.67, sd=0.17) constrained between 0.2 and 1.0, as required for the Beverton-Holt steepness parameter. For the constraint on unfished biomass, I used a Jeffrey's distribution, $P(B_0) \sim \frac{1}{B_0}$, which assigns lower probability to large unfished biomass values (Millar, 2002).

Sensitivity Analyses

Data deficiencies, measurement errors, and knowledge gaps are inherent in all fisheries stock assessments (Maunder and Piner, 2015). Thus, modellers are forced to make a variety of assumptions in estimating parameters of interest. Therefore, it is important to explore the effects of the necessary assumptions and uncertainties through comprehensive sensitivity analyses (Hilborn and Mangel, 1997). I tested model sensitivity to individual survey indices, age at knife-edge recruitment, natural mortality, the penalties for steepness and initial biomass, and the form of the SRR. Unless reported otherwise only one parameter was changed in each sensitivity run, with all other inputs left at the reference case value.

Survey Indices

I tested the sensitivity of the results to individual survey indices by systematically assigning a likelihood weight of zero to each survey in turn and re-fitting the models.

Natural Mortality

Alternative input parameters for M are summarized in table 2. The values for *M* were sourced from Yelloweye stock assessments in Alaska (Olson et al., 2018), and Washington State (Taylor and Wetzel, 2011).

Penalty on Steepness

For the penalized log-likelihood on steepness I arbitrarily chose to vary the standard deviation to make it more or less restrictive (table 2).

Penalty on Initial Biomass

I also attempted to refit the reference case assessment models after replacing the Jeffrey's penalty on B_0 with an exponential penalty parameterized with three different values of λ (table 2).

Age at Knife-edge Recruitment

The influence of different ages for knife-edge recruitment, *k,* were tested for each stock. Because preliminary results showed high sensitivity to the *k* parameter, I expanded the range of values tested (table 3).

Table 2. Fixed input parameter values for natural mortality, *M*, and specifications for penalized log-likelihoods on steepness and initial biomass used for sensitivity analyses in the delay-difference models.

h	*M*	B_0
mean=0.67 sd=0.10	0.02 (Alaska)	$P(B_0) \sim \lambda e^{-\lambda B}$ λ = 0.1, 0.25, 0.5
mean=0.67 sd=0.21	0.046 (Washington)	

Table 3. Range of ages (years) tested in sensitivity analyses on the knife-edge recruitment parameter, *k*. Table headings correspond to the names of the sensitivity runs and are consistent throughout the document.

Stock	Low_*k*	*R*ef_*k*	Mid_*k1*	Mid_*k2*	High_*k*
CW	13	14	18	22	25
N	13	14	18	22	25
S	13	14	18	22	27
NC	13	14	18	22	25
SC	13	15	18	22	25
5E	13	14	18	22	25
5D	14	14	18	22	27
5C	13	13	18	22	27
5B	13	15	19	23	27
5A	12	12	17	21	26
3D	14	14	18	22	25
3C	11	14	18	22	27

Stock-Recruit Relationship

To reduce the number of estimated parameters in the models, I also ran the assessments with an alternative SRR, in which recruitment for each year was set equal to the average unfished recruitment $R_{0,}$ which reduced the estimated parameters to one, by assuming steepness h was equal to one. For the average recruitment SRR, reference points and status indicators were estimated by the following: equilibrium biomass was initialized as (Hilborn and Walters, 1992)

$$G = \frac{1-(1+\rho)S_e+\rho(S_e)^2}{w_k-\rho * w_{k,t-1} * S_e} \tag{18}$$

Where G is a growth survival constant. Equilibrium biomass, B_e was calculated as

$$B_e = \frac{R_0}{G} \tag{18}$$

and equilibrium yield, Y_e, was then estimated using the Baranov catch equation (Eq.1.17).

Results

Biological Data

Weight-at-age plots, estimated from the separate growth analysis for each stock, are included in Appendix A. No major differences in growth were found between stocks, even at the finest spatial scales (Appendix A, figure 1) and stocks in all areas show a consistent downward trend in mean weight during the 1990s (Appendix A, figure 2).

Trends in Abundance Indices

The IPHC survey followed similar trends for all stocks (figure 2), although the range of relative abundance over the time series was smaller in Areas 5D, 3D, and 3C. In general the IPHC and PHMA surveys had similar trends at the aggregate stock scale. However, for some individual PGMAs the relationship between the surveys was more variable. Estimates of catchability *q* and standard deviation *sd* for each survey *i* are reported in table 4, where $sd_i = \sqrt{\frac{\sum (q_i - \overline{q}_i)^2}{n_i}}$ and *n* is the number of survey observations. As expected, catchability was lower for the IPHC than the PHMA surveys.

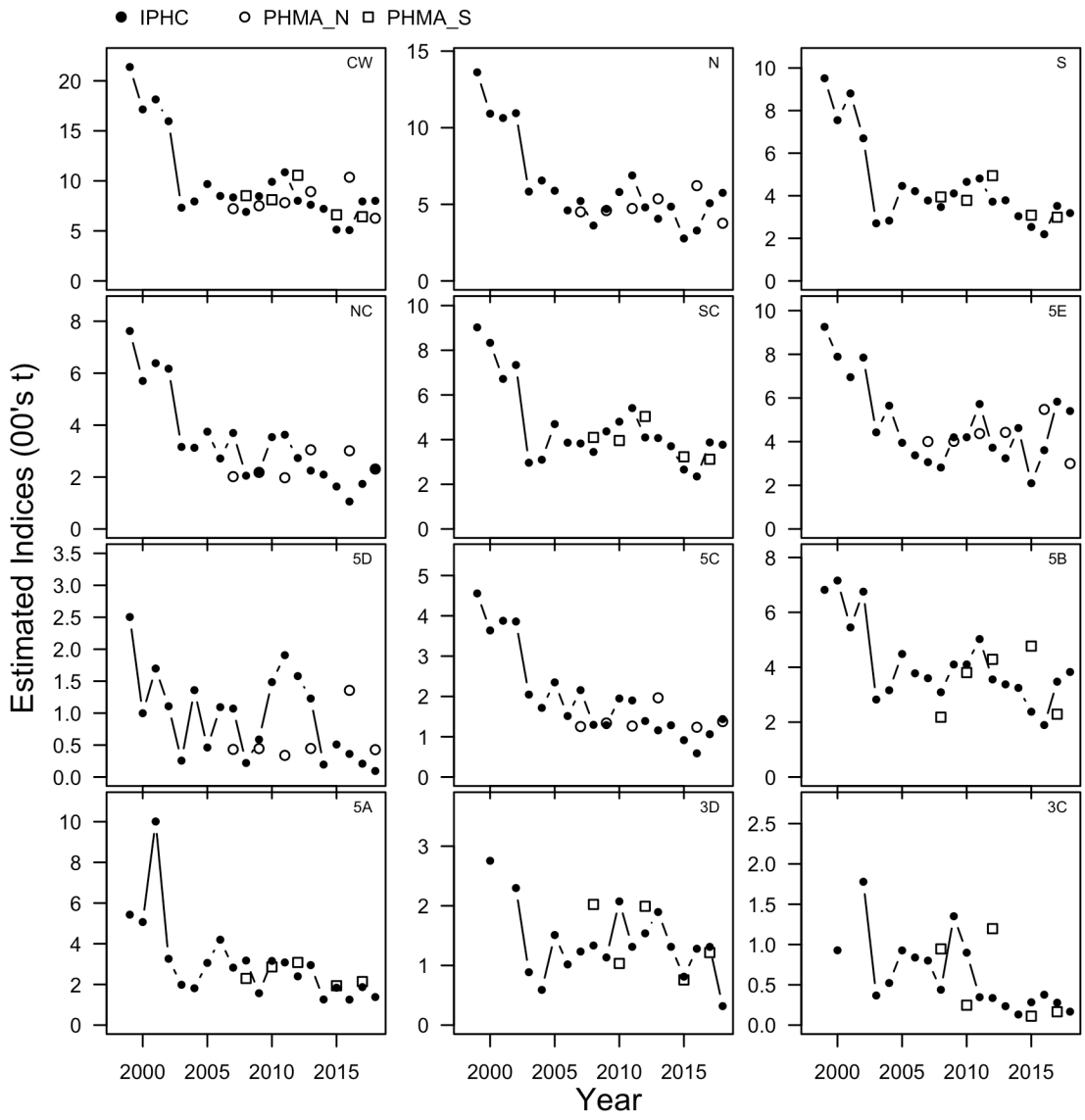

Figure 2. Relative abundance time series for the IPHC, PHMA North and PHMA South long line surveys by stock area.

Table 4. Maximum likelihood estimates for catchability *q,* and survey standard deviation, *sd*, for IPHC, PHMA North and PHMA South long line surveys for each stock.

	Catchability Coefficient (*q*)			Standard Deviation (*sd*)		
Stock	**IPHC**	**PHMA_N**	**PHMA_S**	**IPHC**	**PHMA_N**	**PHMA_S**
CW	3.4E-08	4.71E-05	3.84E-05	0.198	0.175	0.109
N	5.8E-08	7.91E-05	NA	0.225	0.161	NA
S	6.6E-08	NA	7.44E-05	0.221	NA	0.098
NC	5.9E-08	5.97E-05	NA	0.28	0.243	NA
SC	8.2E-08	NA	8.40E-05	0.204	NA	0.082
5E	2.0E-07	2.54E-04	NA	0.284	0.184	NA
5D	8.6E-08	1.61E-04	NA	0.845	0.404	NA
5C	1.2E-07	1.20E-04	NA	0.283	0.196	NA
5B	1.2E-07	NA	1.03E-04	0.225	NA	0.329
5A	8.7E-08	NA	1.68E-04	0.395	NA	0.168
3D	1.7E-07	NA	2.35E-04	0.352	NA	0.421
3C	1.7E-07	NA	6.97E-05	0.448	NA	0.816

Parametric Versus Non-parametric Bootstraps

There were no major differences between the parametric and non-parametric bootstrapped distributions (e.g., figure 3 shows results for the estimated steepness parameter). Therefore, unless otherwise noted, I report only the parametric bootstrap results.

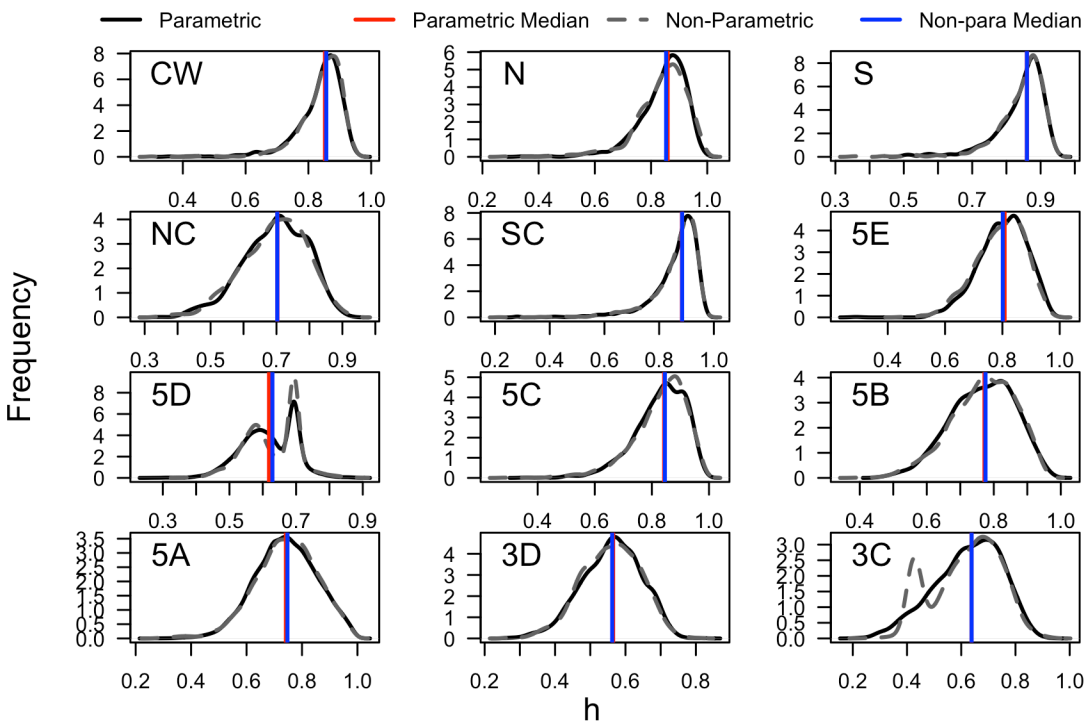

Figure 3. Frequency distributions and median estimates for the steepness parameter *h.* Both parametric and non-parametric bootstrap results are shown for comparison between the two methods.

Reference Case Results

Model convergence was achieved for all stocks, but not all bootstrap iterations. Iterations that failed to converge were dropped from results, along with those where catch exceeded biomass in any year. The number of attempted and successful bootstrap iterations for the reference case is shown for each stock in table 5.

Table 5. Successful bootstrap iterations relative to total attempted iterations for the reference case model runs for each Yelloweye stock. Unsuccessful iterations were those for which *optim* did not achieve convergence, or where catch exceeded estimated biomass in any year of the time series.

Stock	CW	N	S	NC	SC	5E	5D	5C	5B	5A	3D	3C
Successful	1000	1000	1000	1000	4000	1000	5000	1000	1000	8000	2000	4000
Total Boot	1000	1000	1004	1000	4000	1000	6130	1000	1000	8000	2069	4001

For *h,* the effect of the penalty on the bootstrapped frequency distribution was inconsistent between stocks (figure 4). In most cases the asymmetric nature of the penalty's Beta distribution shifted the bootstrapped median estimate of *h* to the right of the mean of the penalty. Three stocks (5D, 3D, and 3C) showed the opposite relationship, where the bootstrapped median shifted to the left of the penalty mean. The bi-modal shape of the bootstrap distribution for 5D (parametric and non-parametric results) and 3C (non-parametric results only) were atypical (figure 3) due to differences between the Beta penalty and the likelihood, which could not be resolved by the data. Re-running the bootstrap procedure for 5D, without the penalty on steepness, resulted in a unimodal distribution and a median *h* of 0. 50, lower than the estimate obtained from the run with a penalty on steepness (0.619).

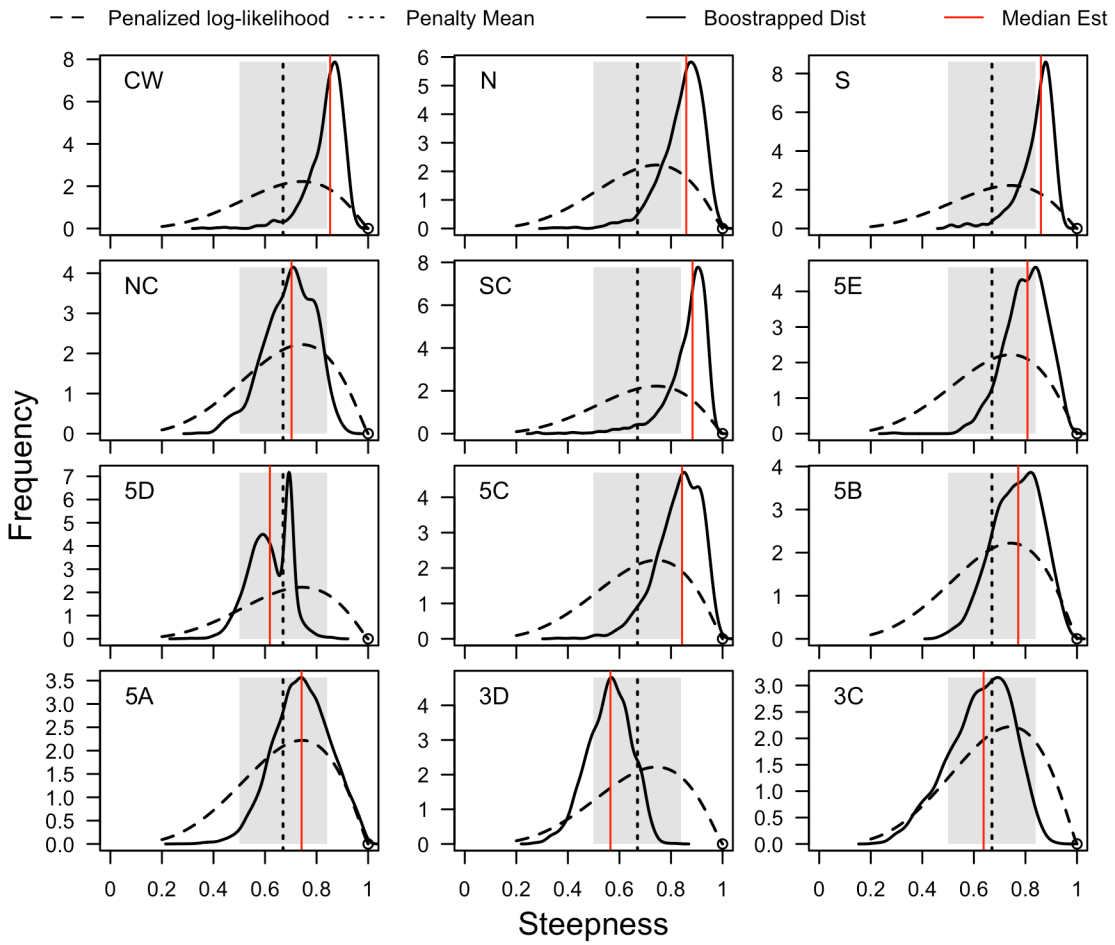

Figure 4. Parametric bootstrapped distributions and penalized log-likelihoods for the steepness parameter *h* for 12 Yelloweye stocks. Vertical lines show the mean of the distribution for the penalized log-likelihood, which was the same for all stocks, and the median estimate from the bootstrap procedure. The shaded area covers the standard deviation around the mean of the penalized log-likelihood. Note that the scale of the y-axis is different for each panel.

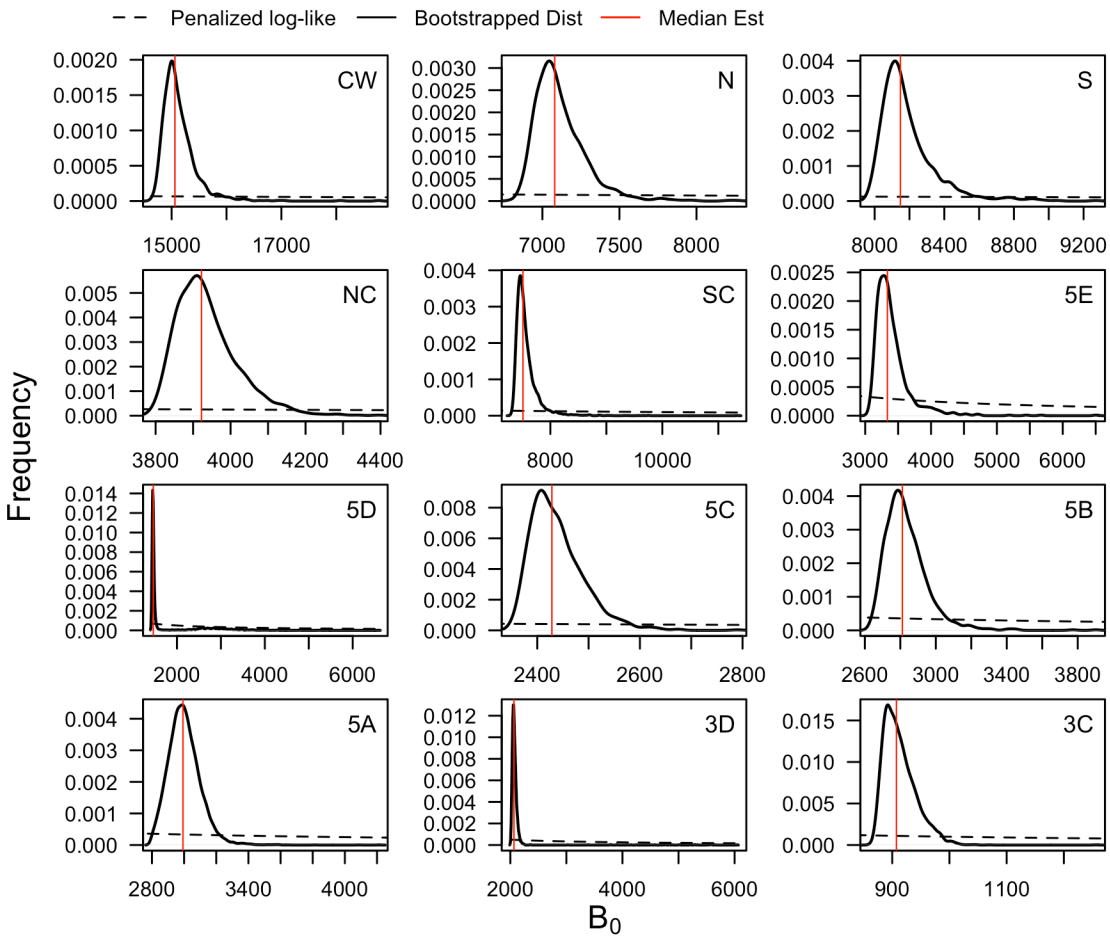

Figure 5. Parametric bootstrapped frequency distributions, and median B_0 estimates for each Yelloweye stock. Jeffrey's penalty on B_0 was uninformative over the range of the bootstrap distribution for all stocks.

Over the range of the bootstrapped frequency distribution for initial biomass the hyperbolic Jeffrey's penalty on B_0 was uninformative for all stocks (figure 5).

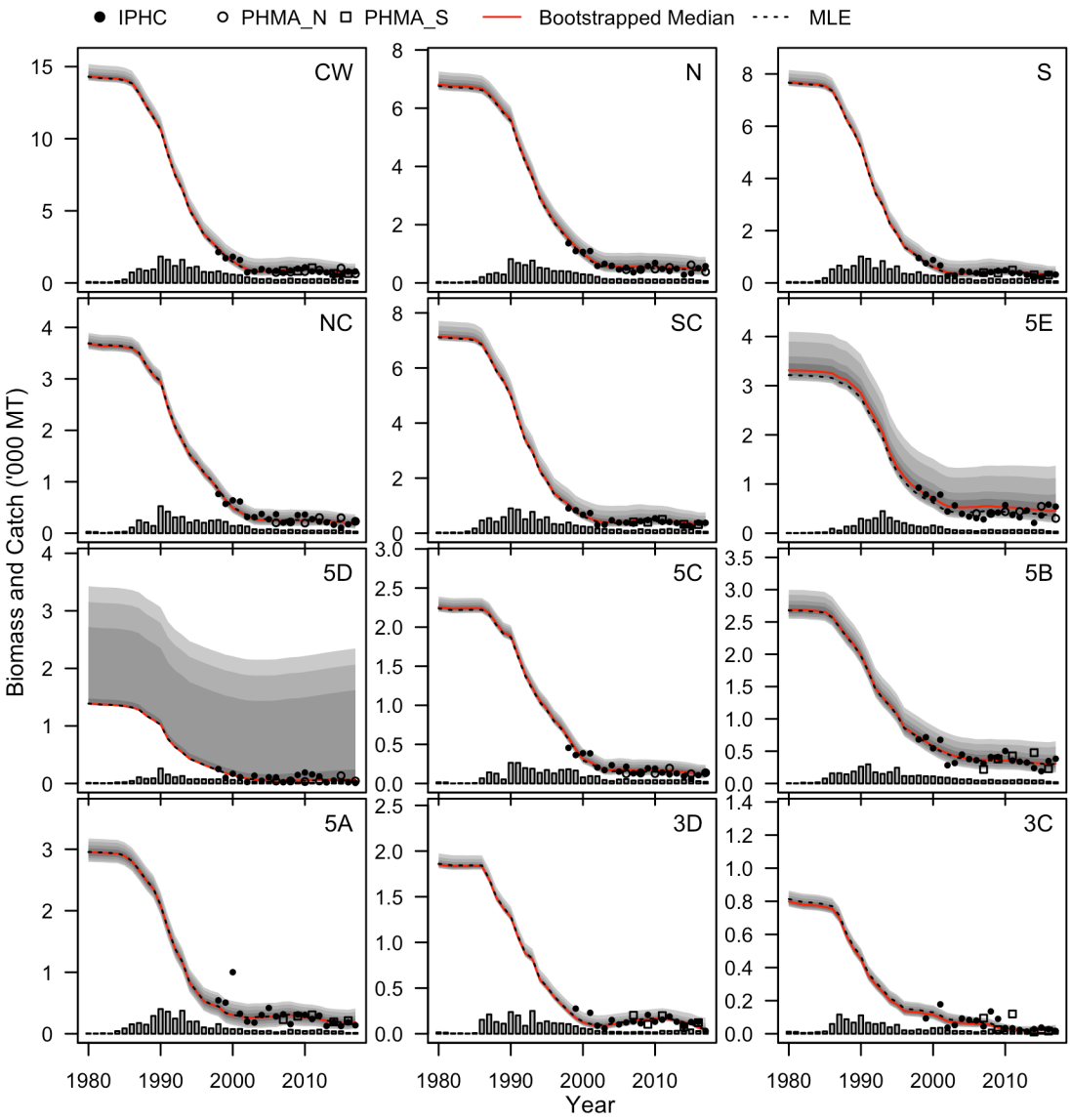

Figure 6. Estimated biomass time series for each Yelloweye stock. Both the MLE and median bootstrap estimated time series are plotted. Catch is shown as vertical bars on the x-axis, and annual survey CPUEs are plotted as points. 50%, 75%, 90% and 95% bootstrapped confidence intervals are shown as polygons in ascending shades of grey. The time series are truncated, as there was relatively little change in biomass prior to the mid-80s.

Qualitative model fits to catch and survey data performed well, in most cases (figure 6). The MLE biomass time series closely matched the median bootstrapped estimate for most stocks, although 5E and 3C showed small differences. All stocks experienced a marked decline beginning in the late 1980s, coinciding with the period of greatest removals. Stock 5D, on the northeast side of Haida Gwaii, had the highest

number of unsuccessful bootstrap iterations (table 5) and the 95% confidence interval shows a disproportionate concentration of mass above the line of best fit.

Median bootstrapped parameter estimates, reference points, and derived quantities from the reference runs are shown in table 6. Median steepness varied by stock, ranging from 0.57 in 3D, to 0.88 in SC. As expected, *MSY* decreased at finer spatial scales, with the lowest estimate of 10 tonnes for area 3C. Generally, stocks with lower *h* had lower estimated values of F_{MSY}. As expected, confidence intervals for *h* get relatively wider as the spatial scale gets more defined (figure 3), although this relationship doesn't hold for B_0 for all stocks (figure 5).

All Yelloweye stocks in my analysis were estimated to be in the critical zone in 2017, except for 5E and 5B which were in the cautious zone (figure 8). Stocks 5D and 5E had very wide bootstrapped confidence intervals. These were the same stocks with the highest variance around estimated biomass (figure 6).

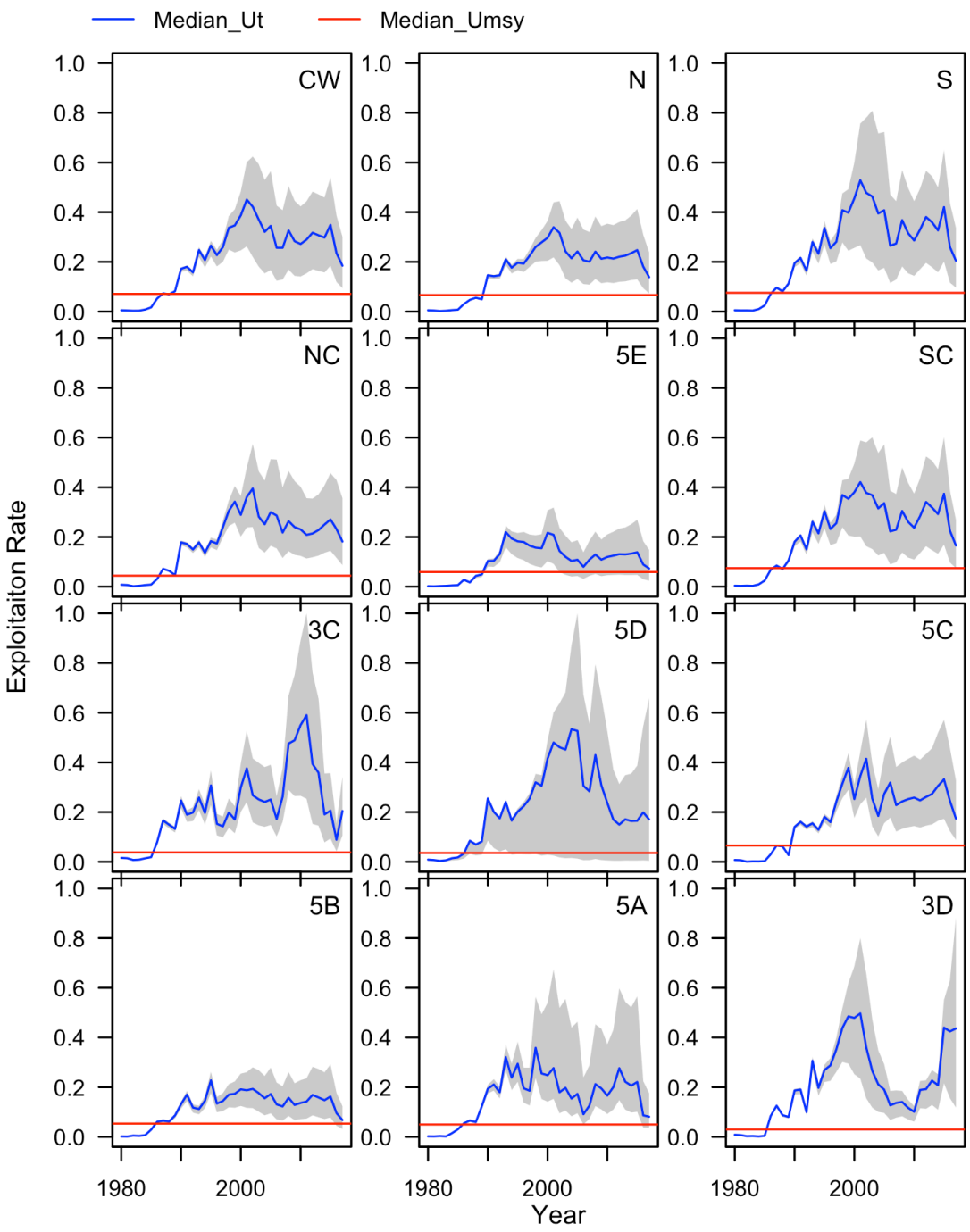

Figure 7. Median estimated harvest rate over time for each Yelloweye stock. Shaded areas represent the 95% bootstrapped confidence interval. The red horizontal line is the median estimate for U_{MSY}.

Table 6. Median parameter estimates, reference points, and derived quantities from the reference runs. 5th and 95th percentiles are shown in parentheses. All biomass values are in tonnes.

Stock ID	*h*	B_0	*MSY*	B_{MSY}	F_{MSY}	B_{2017}/B_0 (%)	F/F_{MSY}
Scenario One							
CW	0.853 *(0.646, 0.927)*	15060 *(14769, 15919)*	240 *(192, 258)*	3379 *(2716, 4846)*	0.075 *(0.041, 0.102)*	4.6 *(2.9, 8.4)*	2.5 *(1.7, 3.6)*
Scenario Two							
N	0.859 *(0.629, 0.954)*	7080 *(6895, 7531)*	108 *(84, 119)*	1629 *(1239, 2314)*	0.070 *(0.037, 0.102)*	6.7 *(4, 11.9)*	2.1 *(1.2, 3.4)*
S	0.860 *(0.636, 0.926)*	8148 *(8004, 8629)*	134 *(105, 144)*	1784 *(1458, 2643)*	0.080 *(0.041, 0.106)*	3.7 *(2.3, 7.5)*	2.6 *(1.7, 3.7)*
Scenario Three							
NC	0.703 *(0.483, 0.852)*	3922 *(3821, 4139)*	50 *(35, 59)*	1133 *(887, 1507)*	0.046 *(0.024, 0.070)*	4.5 *(2.3, 8.9)*	4.1 *(2, 7.4)*
SC	0.883 *(0.619, 0.954)*	7510 *(7365, 8084)*	120 *(91, 129)*	1613 *(1276, 2555)*	0.079 *(0.037, 0.108)*	4.5 *(2.8, 9.5)*	2.1 *(1.4, 3)*
5E	0.808 *(0.624, 0.939)*	3337 *(3128, 4120)*	50 *(39, 60)*	837 *(587, 1164)*	0.062 *(0.037, 0.1)*	13.7 *(7.2, 33.1)*	1.2 *(0.4, 2.4)*
3C	0.638 *(0.362, 0.826)*	907 *(875, 981)*	10 *(5, 13)*	278 *(204, 407)*	0.039 *(0.014, 0.068)*	3.1 *(1.9, 5.8)*	5.3 *(2.3, 15.3)*
Scenario Four							
5D	0.619 *(0.461, 0.751)*	1461 *(1438, 3497)*	17 *(12, 45)*	492 *(403, 1021)*	0.037 *(0.022, 0.053)*	4.3 *(1.1, 67.1)*	4.9 *(0.1, 23.2)*
5C	0.843 *(0.623, 0.955)*	2428 *(2369, 2565)*	37 *(29, 42)*	571 *(414, 803)*	0.069 *(0.037, 0.108)*	5.0 *(2.7, 9.5)*	2.6 *(1.4, 4.5)*
5B	0.772 *(0.574, 0.928)*	2812 *(2668, 3121)*	39 *(31, 46)*	733 *(507, 1012)*	0.056 *(0.032, 0.096)*	11.1 *(6.3, 21.1)*	1.2 *(0.6, 2.3)*
5A	0.742 *(0.526, 0.945)*	2992 *(2836, 3215)*	40 *(29, 49)*	815 *(498, 1118)*	0.052 *(0.028, 0.106)*	6.2 *(3.0, 12.8)*	1.6 *(0.8, 2.8)*
3D	0.565 *(0.385, 0.704)*	2066 *(2022, 2195)*	21 *(13, 27)*	697 *(582, 911)*	0.031 *(0.016, 0.046)*	2.3 *(1.1, 8.1)*	14.4 *(3.7, 30.9)*

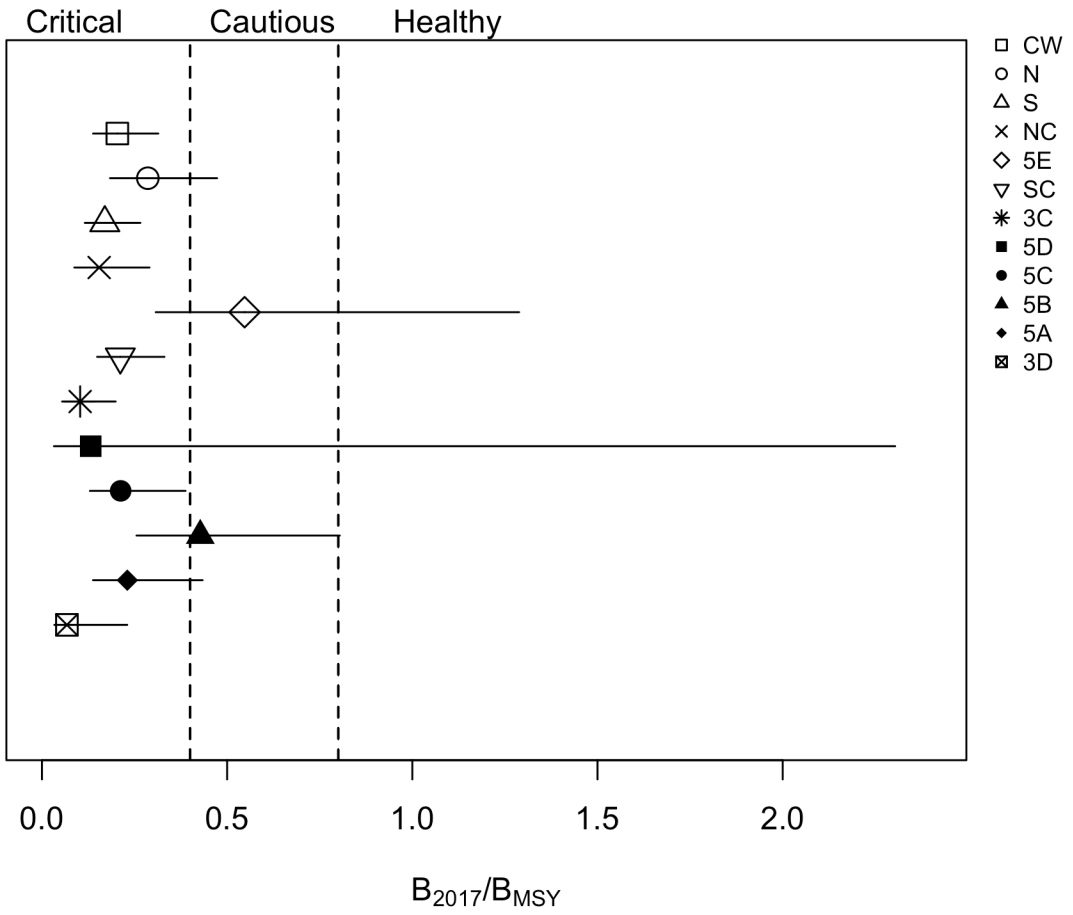

Figure 8. Estimated stock status in 2017. Yelloweye stocks are arranged generally in order of spatial scenarios i.e. the first scenario, the coast-wide stock is plotted first. Horizontal lines indicate 95% bootstrapped confidence intervals and dashed vertical lines demarcate the critical, cautious, and healthy status zones.

The median bootstrapped biomass time series for each aggregate stock and its component stocks aligned very closely in most cases (figure 9). Differences between aggregate and summed estimates were more pronounced when the south aggregate was split into its four component stocks, and when the coast wide stock was split into the seven PGMAs. In these two cases the sum of the biomass for the smaller stocks exceeded the biomass of the aggregate stock (panel 5).

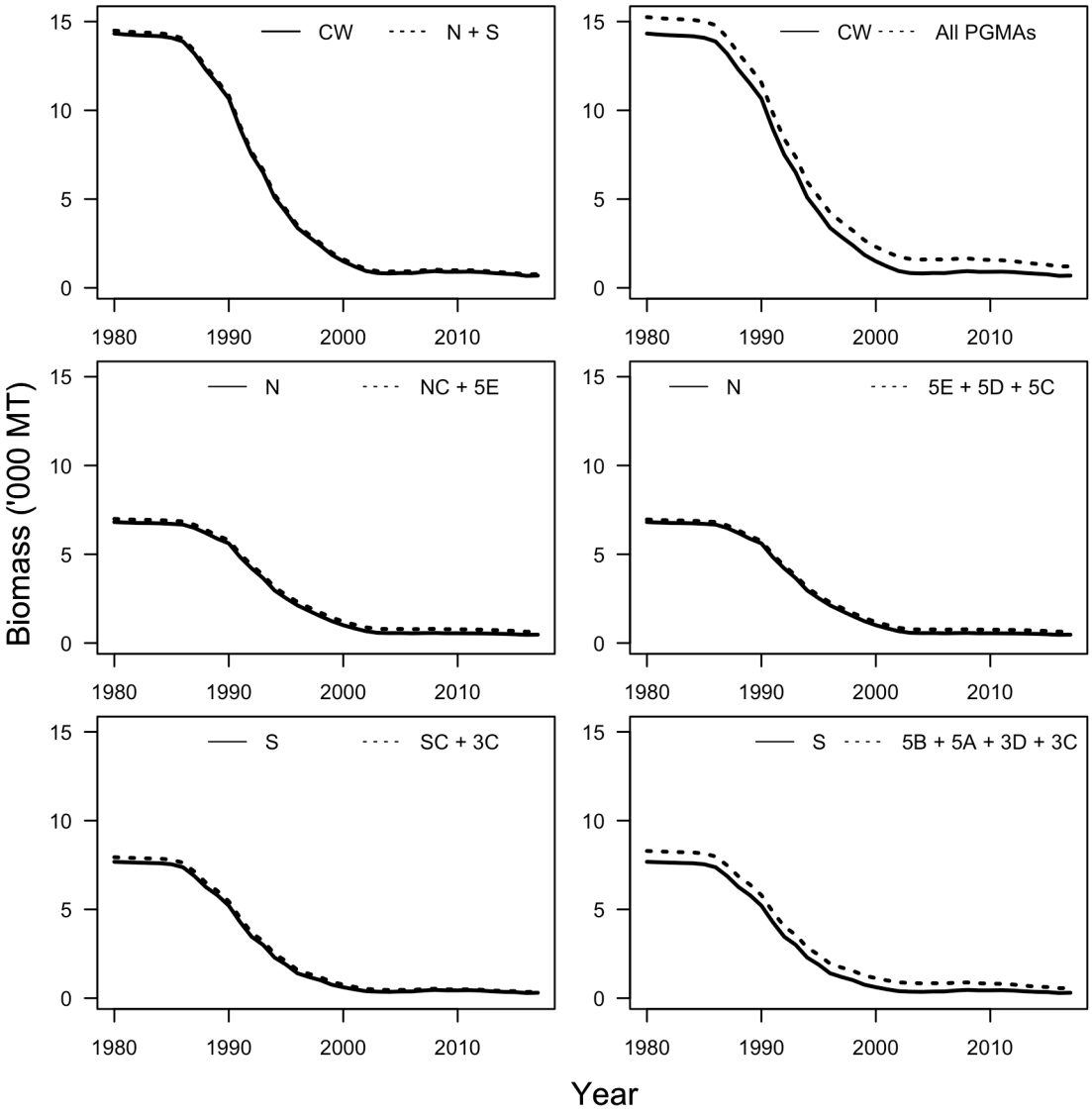

Figure 9. Median estimated biomass time series for each aggregate stock and the summed estimated biomass of its components stocks. Refer to figure 1 for the map showing spatial breakdown of aggregate stocks into component stocks. Time series have been truncated.

Sensitivity Analyses

Key results for each type of sensitivity analysis are summarized here, while detailed tables of estimated parameter values and management quantities of interest are included in Appendix B. Model convergence was assessed for each iteration and numbers of successful versus total bootstrap iterations are reported in table 1 (Appendix B). There were no major differences in bootstrap success relative to the reference case

runs, and the stocks with large numbers of dropped runs remained consistent across analyses (e.g. 5D).

Survey Indices

Model sensitivity to each survey index was assessed for each stock (figure 10). The MLE biomass time series from each reference run, in which models were fit to both IPHC and PHMA indices, aligned closely with the IPHC survey results for all stocks. On the coast-wide scale, the fits to the PHMA South survey gave similar results to fits from the IPHC. Fits to the PHMA North resulted in higher biomass for the coast-wide, North, 5E, and 5C stocks. Fits were more similar between the IPHC and PHMA South than between fits to the IPHC and PHMA North. The NC stock showed smaller estimates of biomass when fit to the PHMA North survey.

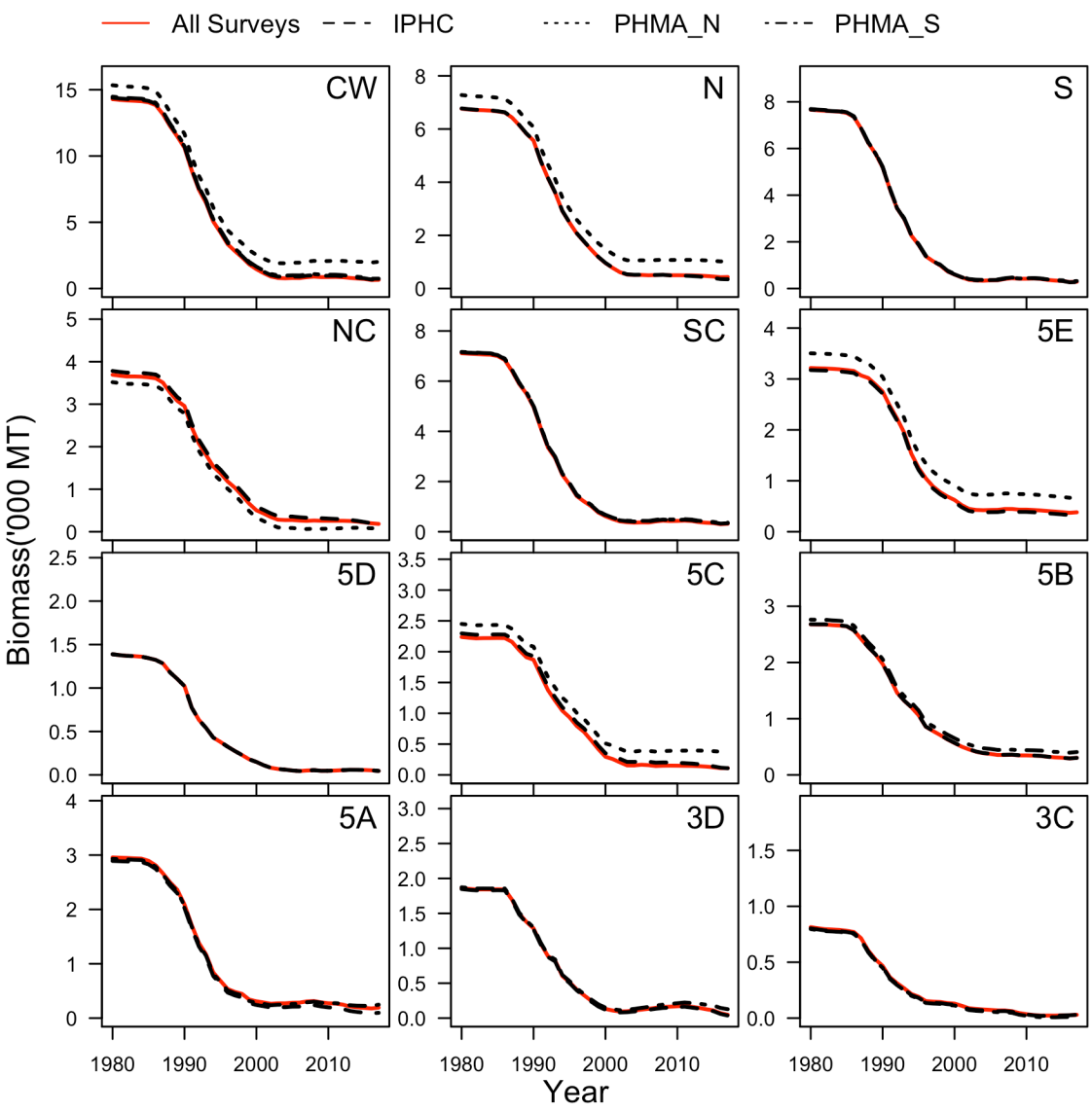

Figure 10. MLE biomass time series for each Yelloweye stock from sensitivity analyses on model fits to individual relative abundance indices. Results from the reference case, where stocks were fit to all survey indices are shown for comparison.

Penalty on Steepness

The mean of the steepness penalty was kept constant for all sensitivity analyses while the standard deviation was varied to make it more or less restrictive. In general, higher standard deviation on the penalty resulted in higher median estimates of steepness (figure 11 and Appendix B, tables 3 and 4), although there were some exceptions, such as SC, where the median decreased. Reducing the penalty standard

deviation resulted in median estimates of *h* that were closer to the penalized mean, relative to the reference case; once again with the exception of SC. There was no significant change in median *h* for 5D, 3D, or 3C as a result of changing the standard deviation, and estimates for these stocks remained close to the mean of the penalty on steepness.

The effect on annual abundance estimates was small, but B_{MSY} and F_{MSY} were sensitive to changes in the standard deviation of the penalty on steepness. The 95% bootstrapped confidence intervals for B_{MSY} and F_{MSY} were broad for most stocks, regardless of the standard deviation on the penalty (table 6 and Appendix B, tables 3 and 4). Model conditions that resulted in higher estimates of *h* gave correspondingly higher estimates of F_{MSY}, which is known to be an increasing function of *h* (Brooks et al., 2010; Mangel et al., 2013). Perceptions of stock status relative to the three status zones (critical, cautious, and healthy) did not change over the range of steepness sensitivity analyses examined for any stock (figure 12).

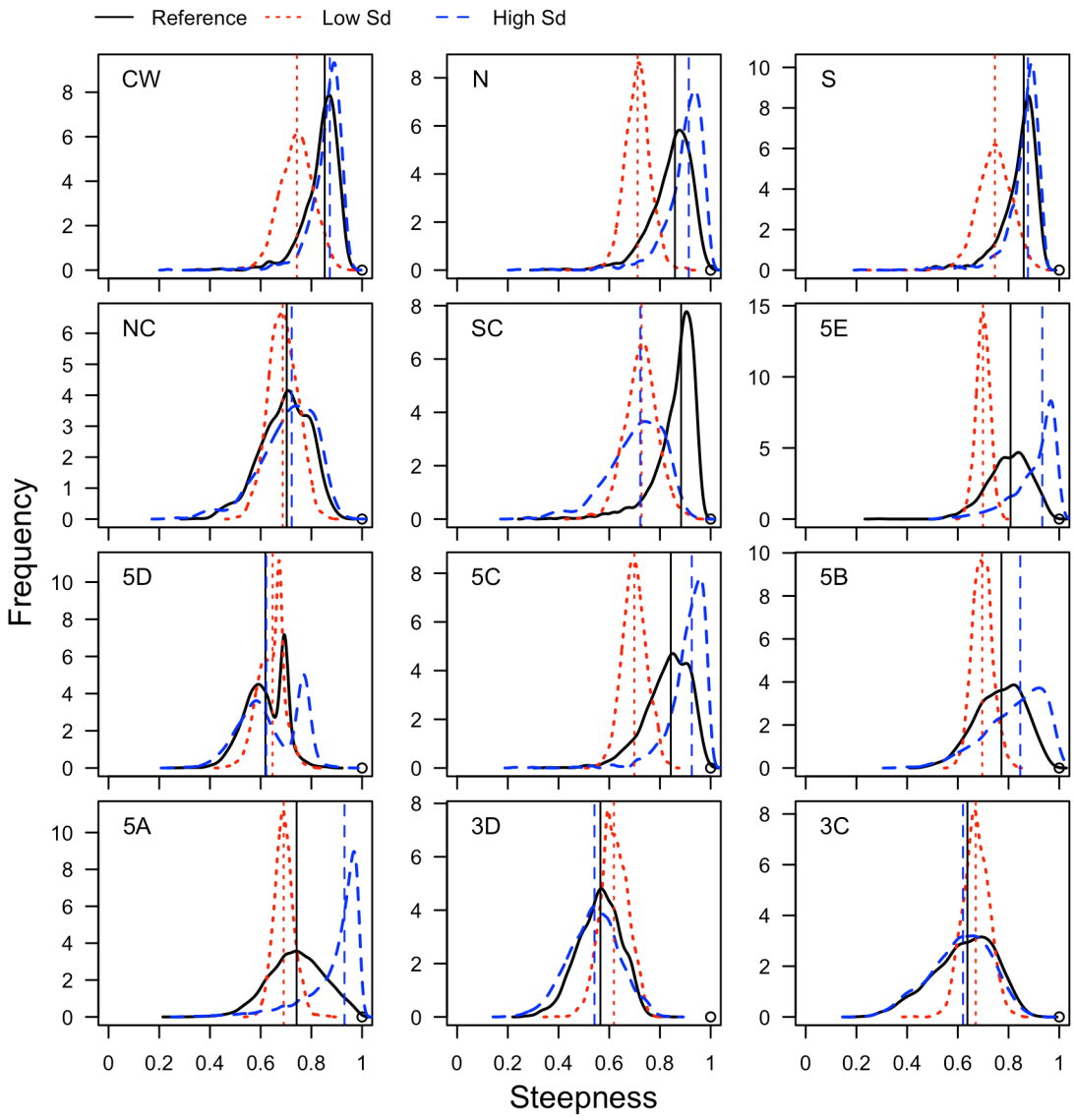

Figure 11. Frequency distributions for bootstrapped estimates of the steepness parameter *h* with a mean of 0.67 and low (0.11), reference (0.17), and high (0.21) values for standard deviation of the penalized log-likelihood. Vertical lines show the median steepness estimate for each of the low, reference, and high scenarios.

Exponential Penalty on Initial Biomass

As an alternative to the Jeffrey's penalty on B_0, used in the reference case, I attempted fitting the models with an exponential penalty, with three different λ values (table 2). Attempts to fit these models were unsuccessful for all Yelloweye stocks. Regardless of the value of λ, the estimated biomass for all stocks was unreasonably low, with values lower than catch in many cases.

Natural Mortality

Reducing the fixed value of *M* resulted in smaller median estimates of *h* and larger estimates of B_0 (Appendix B, table 5). Increasing *M* resulted in smaller median *h* for most stocks, but also smaller B_0. F_{MSY} varied either up or down, depending on the stock, but tended to decrease relative to the reference case (Appendix B, table 6). Low natural mortality gave higher estimates of B_{MSY} and lower estimates of *MSY* for most stocks, while the higher *M* had a smaller effect on these two reference points. Reducing natural mortality altered estimated stock status relative to $0.4B_{MSY}$, but only for the north (N), and 5E stocks (figure 12). Stock 5B shifted slightly, but remained within the cautious zone. Conversely, increasing natural mortality changed estimated stock status for the 5D and 5B stocks.

Age at Recruitment

The lowest value of *k,* estimated from the analysis of length and age data for each stock*,* had very little effect on model estimates overall, and resulted in no change to estimates of current stock status (figure 12). However, the high *k*, which was more than 10 years greater than the reference case for most stocks, had a significant effect on stock status. At high values of *k,* status in 2017 improved dramatically for most stocks, except 5E and 5B (figure 12). The apparent sensitivity to *k* prompted me to test two more ages between the derived reference and high (high_*k*) ages-at-recruitment. The additional selected *k* values were meant to roughly divide the difference between the reference and high *k* (table 3).

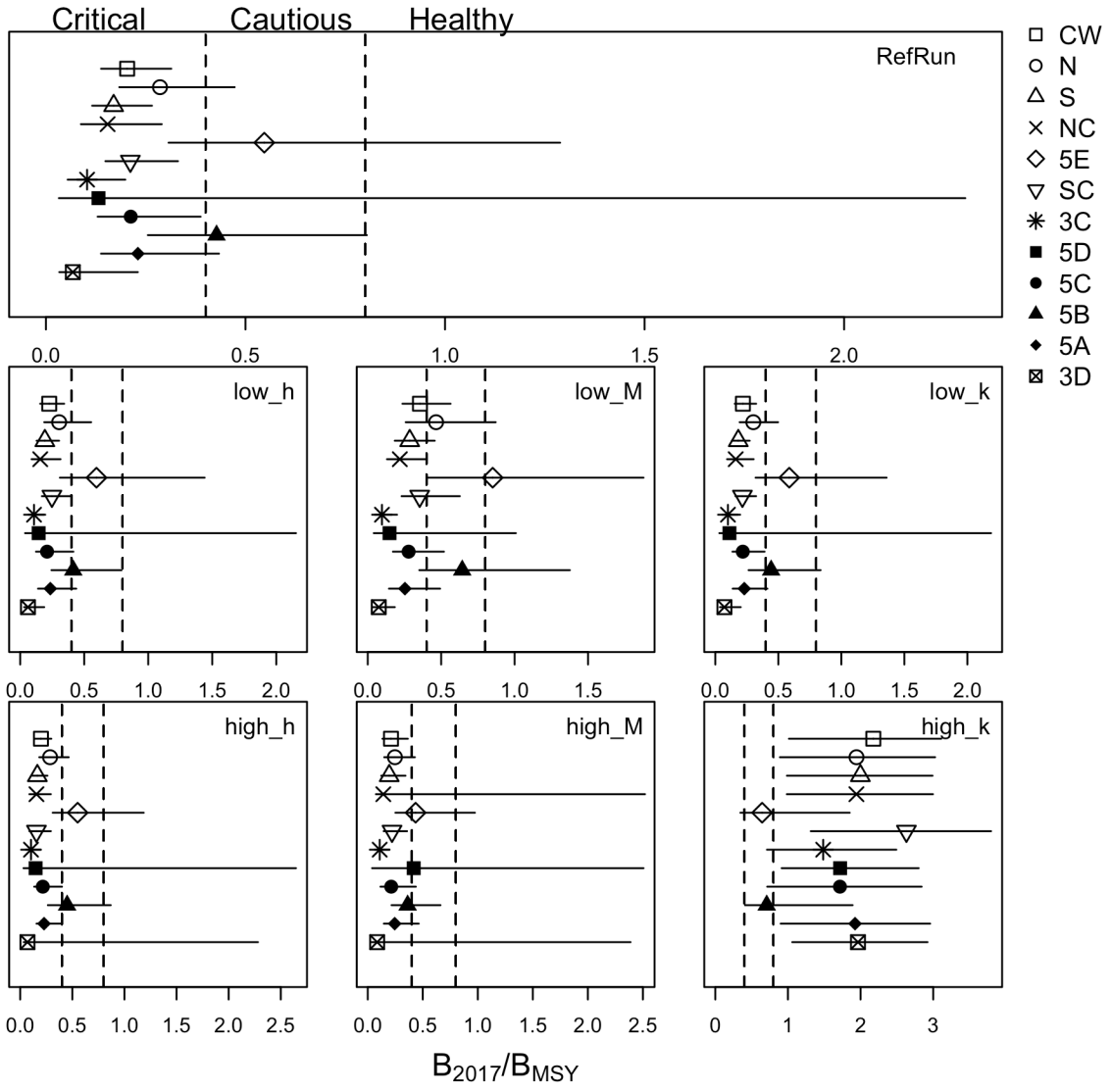

Figure 12. Changes to stock status in 2017 as a result of sensitivity analyses on the penalty for steepness (low_*h* and high_*h*), fixed natural mortality rate (low_*M* and high_*M*), and age at knife-edge recruitment (low_*k* and high_*k*). Yelloweye stocks are arranged generally in order of spatial scenarios i.e. the first scenario, the coast-wide stock is plotted first. Reference case results are shown in the top panel for comparison. Input parameters for the sensitivity analyses are reported in table 2. 5th and 95th percentiles are shown as horizontal bars.

Under the additional values of *k* (mid_*k1* and mid_*k2*), status for 5D and 3D shifted under the mid_*k1* scenario (figure 13) while the rest of the stocks shifted in the mid_*k2* scenario. Stock status in 5E and 5B shifted between the critical and cautious zones, but were less sensitive to changes in the *k* parameter relative to the other stocks that all shifted from critical to healthy.

For the mid_*k2* and high_*k* scenarios there were large differences between MLE and bootstrapped median biomass time series and, visually, model fits degraded (fits not shown). Natural mortality can be confounded with other important parameters, including selectivity (Punt et al., 2002; Crone and Valero, 2014). To assess the interaction between *k* and *M* for the models parameterized with higher *k* values, I performed an additional analysis where I refit the mid_*k2* and high_*k* models with the low natural mortality rate of 0.02 yr^{-1}, instead of the reference *M* of 0.038 yr^{-1}. This stabilized the model behaviour and resulted in better visual fits (not shown). The mid_*k2*, low *M* models resulted in higher estimates of abundance relative to the reference cases but, for most stocks, status in 2017 was basically the same as for the reference case runs.

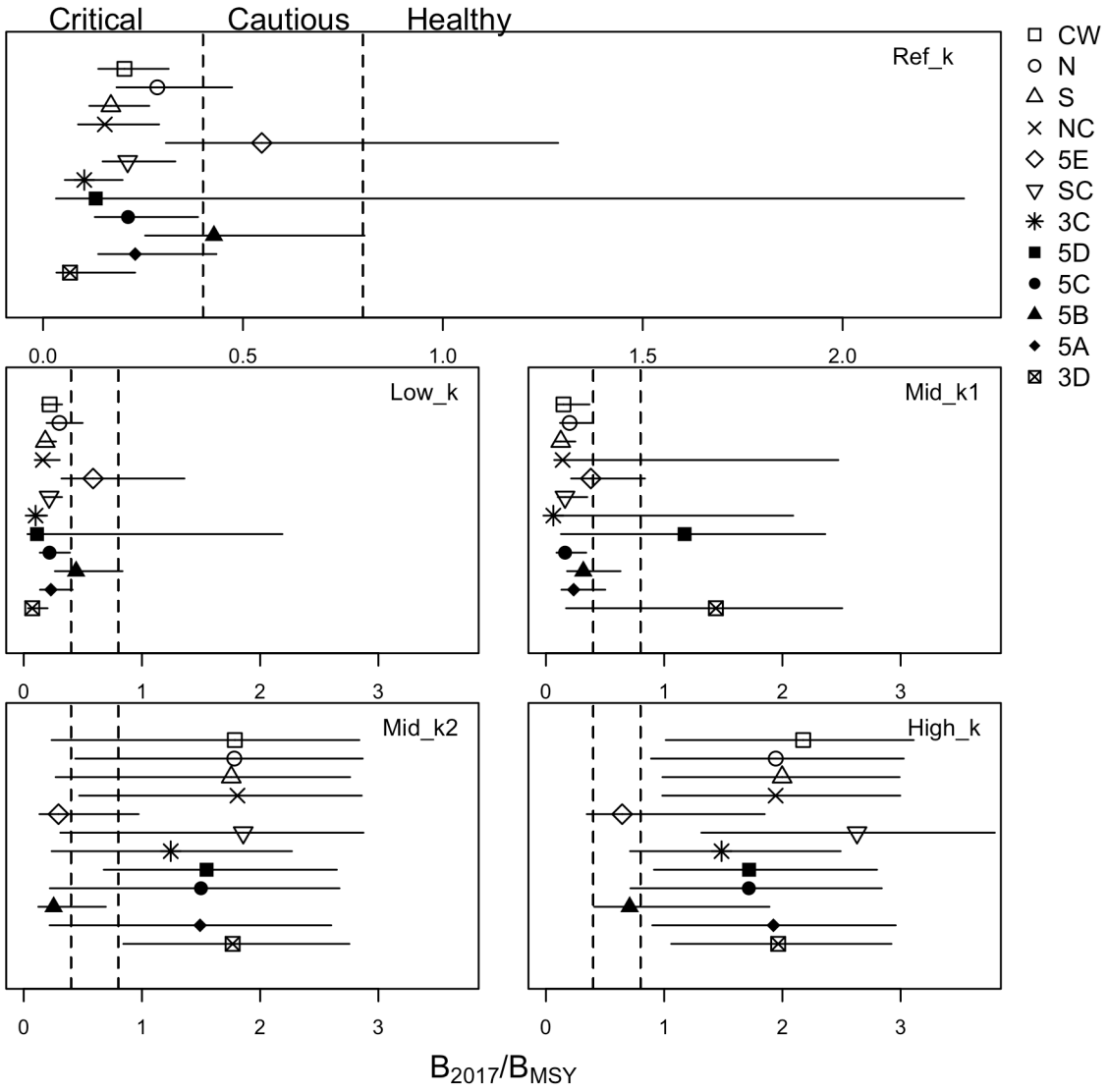

Figure 13. Changes to stock status in 2017 as a result of sensitivity analyses on age at knife-edge recruitment, *k,* for each Yelloweye stock. All other input parameters were kept the same as for reference case runs. Yelloweye stocks are arranged generally in order of spatial scenarios i.e. the first scenario, the coast-wide stock is plotted first. The 5th and 95th percentiles are shown as horizontal bars. Reference case results are shown in the top panel for comparison.

Stock Recruitment Relationship

Results for the average recruitment relationship, wherein annual recruitment was equal to the estimate of initial recruitment for the length of the modelled time series, are shown in Appendix C. I expected the average recruitment results to be approximately the same as the Beverton-Holt results because the decline in Yelloweye abundance

happened quickly and it is unlikely that recruitment compensation would have occurred over that time span. Thus, average recruitment should have continued. Overall, the average recruitment SRR gave a slightly more optimistic view of Yelloweye status relative to the Beverton-Holt.

Discussion

The choice of spatial scale for fisheries stock assessment could have important consequences for fishery sustainability. In this paper, I tested delay-difference assessment models over a wider range of spatial scales than they have previously been used in Yelloweye rockfish assessments. Under the assumption of closed populations, the sum of estimated biomass for each sub-stock was roughly equal to the sum of the estimated biomass for the aggregate stock. Estimates of stock status also differed at increasingly finer spatial scales, which supports the hypothesis that Yelloweye may be spatially segregated rather than a single homogenous coast-wide stock. My analysis provides insights that could be useful for development of spatially explicit assessments or other management adjustments for Yelloweye.

One concern with incorporating spatial structure into stock assessments is that, by disaggregating the existing data amongst sub-stocks you reduce the data available to each model, resulting in greater uncertainty and increased risk of bias in assessment results (Chen et al., 2003; Punt, 2019; Berger et al., 2017). There was no evidence of this data scarcity effect in my results for the north south split (i.e. Scenario 2 in figure 1), as there was no substantial increase in uncertainty imposed by disaggregating the coast-wide data into independent north and south stocks. North and south stock models had comparable estimates of productivity, with a similar range of uncertainty as the coast-wide model. There was no increase in precision around estimates of h, F_{MSY}, depletion, or other derived quantities for north and south models, relative to the coast-wide model, but no loss in precision either.

If productivity and initial abundance are similar between areas, historical fishing patterns are likely responsible for differences in stock status at different spatial scales (Booth, 2000). Time series of harvest rates show that fishing effort has not been homogenously distributed along the coast (figure 7). This could have important implications for Yelloweye management because of their long life, late age-at-maturity, and sedentary nature, which makes re-establishment of pre-exploitation structure more drawn out (Ciannelli et al., 2013). For example, median estimates of B_0 and h were similar between the west (stock 5E) and east coasts of Haida Gwaii (stock NC), but depletion and stock status in 2017 differed between the two stocks, with NC being more

depleted relative to 5E. The difference in status is likely a result of the higher harvest rate experienced by the east coast stock versus the west. Fishing effects on population structure may be more pronounced when there is little movement of mature adults (Cianelli et al., 2013) and, as adult Yelloweye are sedentary, if harvest continues to be heterogeneous, differences in stock status between NC and 5E could be amplified over time.

Some of the assessments on the PGMA scale had high uncertainty in stock status estimates, due to data scarcity and or conflicting data. For example, 5D had one of the lowest levels of commercial catch over the time series and a low sampling rate by research surveys, the latter of which may be why I was unable to achieve good model fits for this stock. However, stocks 3C and 3D also had less data than other PGMAs, and their fits were better. I expected that uncertainty would generally increase as a result of splitting the data (Cope and Punt, 2011). Visual inspection of the 95% confidence interval of the estimated biomass time series showed they tended to get wider at the PGMA scale, relative to the coast-wide stock, though not for all stocks.

A compelling argument in favour of finer scale stock delineation for assessment purposes is the concern that the alternative approach, in which data is pooled over multiple stocks or sub-stocks could mask the occurrence of localized depletion (Berger et al., 2017). Likewise, there is concern that the aggregated assessments could mask more productive stocks, leading to lost economic opportunities (Holland and Herrera, 2010). My results show evidence of both conditions occurring for Yelloweye. While the absolute values of depletion reported here underestimate the biomass, because recreational catch is unaccounted for, useful comparisons of the relative depletion between stocks can still be made. At finer spatial scales some Yelloweye stocks were more depleted than indicated by the coast-wide, or aggregate stock estimates. For example, the estimated depletion for the aggregate south stock was 3.7%, but depletion of 3C, a southern sub-stock, was 2.3%. 5E and 5B, in the north and south aggregates respectively, are both less depleted than their aggregates, and were in the cautious status zone instead of the critical zone. However, research has shown that knowledge like this doesn't necessarily mean better management could be achieved at these finer spatial scales. For example, in a simulation study, Holland and Herrara (2010) found that, if fishing mortality was low relative to F_{MSY}, aggregate management of discrete stocks had better economic and conservation performance than area-specific

management because fishermen naturally directed their fishing effort towards more abundant stocks. Under the current management approach for Yelloweye the TAC has been steadily declining (DFO, 2017). Adequate management, in terms of trade-offs between conservation and harvest, may be achievable at aggregate scales under low harvest rates because fishermen will instinctively avoid low productivity areas, saving managers from additional uncertainty associated with refining the scale of assessments.

Stock productivity is an important consideration for sustainable management of harvested species (Jardim et al., 2018) (e.g., less productive stocks would require reduced exploitation relative to more productive stocks in order to ensure long-term sustainability). Productivity is also a key determinant of recovery capacity for depleted stocks (Thorson et al., 2018). For threatened species, like Yelloweye, DFO is required to develop rebuilding plans to grow the stock out of the critical zone within a specified timeframe (DFO, 2009). Setting timelines for rebuilding stocks under different management options relies on having reasonable estimates of productivity for the stock in question. Estimated depletion for all stocks was less than 20% for all reference case and *h* sensitivity runs. It is at such low relative biomass that we expect to learn the most about *h*, which is defined at depletion of 20% of initial biomass (Mace and Doonan, 1988). Some of the median estimates for steepness seemed high, relative to estimates for Yelloweye (0.417, in Taylor, 2011), and other rockfish species (0.75, in Thorson et al., 2018) in Washington State, but 95% confidence intervals were large in all cases considered. The data for all stocks conforms to what is known as a “one-way-trip”, in which there is no contrast in the data to assist in fitting the models (Hilborn and Walters, 1992). The data essentially contain no information on the shape of the SRR curve at low levels of spawning biomass, making it difficult to confidently estimate *h* (Thorson et al., 2018), regardless of the spatial scale of the assessment.

Despite the difficulties with estimating *h,* it is not advisable to fix both the steepness and natural mortality parameters in a stock assessment (Mangel et al., 2013), yet using a fixed value for natural mortality simplified my estimation procedure. I used the best estimates of natural mortality available for reference case model runs and sensitivity analyses. However, fixing *M* can introduce difficulties in interpreting stock assessment results. Delay-difference models will offset changes in the input value for natural mortality by adjusting the estimate of fishing mortality. The model uses data from the relative abundance indices and catch to estimate total mortality and adjusts

estimates of fishing mortality based on the difference between total and natural mortality. It is not uncommon to get similar model fits over a range of *M* with different estimates of *F* and F_{MSY} (Clark, 1999). This describes the behaviour of my model under sensitivity tests on *M,* where abundance estimates were somewhat similar, but estimates of F_{MSY} varied more considerably.

The results of my sensitivity analyses highlight the importance of using the best available data when deciding on values for fixed input parameters for the delay-difference model. Stock status in 2017 was most sensitive to increases in the assumed age-at-recruitment parameter, which shifted most stocks from the critical to the cautious zone between *k* of approximately 18 to 22. The improvement in stock status was a result of the delay-difference model's ability to predict mean weight in the recruited population. Fish will weigh more when they recruit to the fishery at older ages. Weight-at-age of recruitment influences the estimate for initial numbers of fish and also adjusts the annual recruitment, which then determines the estimated biomass. As *k* increases there is also a reduction in the years of data available for estimating recruitment, which increases the uncertainty in the feedback between catch and recruitment. This is evident in the increased width of the 95% confidence intervals on the status plots scenarios with higher *k*.

Selectivity, which in the delay-difference model is the *k* parameter, can be confounded with other important parameters, such as natural mortality (Punt et al., 2002; Crone and Valero, 2014). The results of the mid_*k*2, low *M* sensitivity analyses, where lowering the natural mortality rate stabilized the fits to the delay-difference model, demonstrated that equally good qualitative fits could be achieved from a range of input parameters. Thus it is not only important to use discretion when choosing fixed input parameters, it is also important to interpret delay-difference model results with caution.

Several key uncertainties and assumptions were not explored in my sensitivity analyses. For example, I did not consider ageing error when deriving estimates for age-at-recruitment and other growth parameters from an analysis of Yelloweye length and age data. The biological samples I used were also collected after large declines in spawning stock biomass had occurred. As a result, age and length composition of these samples may not be reflective of the historical Yelloweye population, given that fishing

pressure can alter these population attributes (Berkeley et al., 2004) and this may have introduced bias to the models.

My results from the delay-difference assessment models rely heavily on historical catch. The decision not to include recreational and indigenous catch in my models is a substantial source of bias, affecting estimates of initial biomass and all derived quantities that rely on estimated biomass, such as stock status. However, my model estimated that the coast-wide stock is in the critical zone in 2017 and the DFO assessment in 2014 estimated the same (Yamanaka et al., 2015), so it is likely that the relative status of other stocks would be similar with or without recreational catch. Additional bias could be introduced to the models from my reliance on reconstructed catch. It is probable that there are errors in how reconstructed catch is assigned to various PGMAs, due to factors such as remoteness and inconsistent knowledge of historical catch. Cope and Punt (2011) used simulation experiments to assess the impacts of variable catch history on spatially explicit depletion estimates and found that results were very sensitive to catch history, if management and population scales did not match. However, the focus of this research was to assess the relative differences between areas and any changes I made to the ratios of catch between PGMAs would have been entirely subjective.

Treatment of relative abundance indices can also introduce bias to assessment results (Maunder et al., 2006). IPHC survey data were shown to have a strong influence on abundance estimates, likely because of the length of the time series relative to the other two surveys. For the IPHC data I calculated mean CPUE per year by area, or number of Yelloweye caught per effective skate. I performed no further analysis on the survey CPUEs. The only attempt that I made to account for changes in survey design over the time series was scaling the CPUE by hooks observed, which varied between all hooks, and only the first 20 of each skate. Thus IPHC data between years are not comparable as raw indices. The last DFO assessment used a multinomial exponential analysis to develop CPUE indices for both the IPHC and the PHMA surveys (Yamanaka et al., 2018), which allowed them to control for empty hooks and competition for hooks between species. My treatment of IPHC data was not as rigorous. However, assessing relative trends between areas was the main goal of this research and my treatment of survey indices should be sufficient to capture those trends.

Improving stock assessments by incorporating spatial data may depend on our ability to correctly identify the actual population structure (Goethel and Berger, 2017). For pragmatic reasons, I made several broad, and probably unrealistic, assumptions about the spatial structure of the Yelloweye population and the form of connectivity between stocks. Aligning the boundaries for my stocks with existing management units, such as the boundaries of PGMAs and the extent of PHMA survey coverage, greatly simplified the disaggregation of the data into individual stocks. The assumption of no connectivity or movement between stocks, even during larval stages, further simplified the analysis, but is probably an inaccurate assumption. Even though larval exchange between areas is estimated to be low (Yamanaka et al., 2006), it may still influence differences in abundance between any true sub-stocks.

The objective of this research was to compare results from assessments performed at progressively smaller spatial scales, which could then be used to assess whether the possibility for discrete Yelloweye stocks could safely be ignored in management decisions. My results show that, in some scenarios, uncertainty in stock assessment outputs may be no greater at finer spatial scales than for an aggregate stock (e.g., the north south models versus the coast-wide model), and that there is evidence of differences in stock status at finer scales. However, my results do not mean that managing for spatial structure is necessary to achieve better outcomes for Yelloweye. Current reductions in TAC and avoidance behaviour by fishermen may be enough to ensure recovery in the long term, but it may be several years before we can assess the effectiveness of current management approaches. In the meantime, my results suggest that it might be worthwhile to establish methods for tracking Yelloweye on a finer spatial scale. Especially given that Canada is committed to a precautionary approach to managing fisheries in the face of uncertainty (DFO, 2006).

Ultimately, any decision to switch to finer scale management involves making trade-offs between the potential consequences of ignoring spatial structure and investment of limited resources available for management. In the case of Yelloweye, only a small amount of additional effort would be required to include a northern and southern stock in the next assessment. For example, it is convenient that the PHMA survey already divides sampling into north and south regions and assessment information for each area should improve, as the time series gets longer. Recreational catch could also be resolved to north and south spatial scales and disaggregating the

rest of the input data for the delay-difference model to north and south stocks was straightforward. Comparisons between the aggregated, coast-wide stock, and disaggregated north and south assessments would allow tracking of any differences in responses to management, providing additional certainty regarding management options and potentially leading to improved outcomes for the species. In turn, this could benefit the entire integrated groundfish fishery, by alleviating some of the constraints imposed by Yelloweye conservation measures.

References

Berger, A. M., D. R. Goethel, P. D. Lynch, T. Quinn II, S. Mormede, J. Mckenzie, and A. Dunn. 2017. Space oddity : The mission for spatial integration. Canadian Journal of Fisheries and Aquatic Sciences 74:1698–1716.

Berkeley, S. A., M. A. Hixon, R. J. Larson, and M. S. Love. 2004. Fisheries sustainability via protection of age structure and spatial distribution of fish populations. Fisheries Management 29(8):23–32.

Beverton, R. J. ., and S. J. Holt. 1957. On the Dynamics of Exploited Fish Populations. Chapman and Hall, London.

Booth, A. J. 2000. Incorporating the spatial component of fisheries data into stock assessment models. ICES Journal of Marine Science 57:858–865.

Brooks, E., J. E. Powers, and E. Coetes. 2010. Analytical reference points for age-structured models application to data-poor fisheries. ICES Journal of Marine Science 67:165–175.

Cadrin, S. X., and D. H. Secor. 2009. Accounting for Spatial Population Structure in Stock Assessment : Past , Present , and Future *:405–426.

Chen, Y., L. Chen, and K. I. Stergiou. 2003. Impacts of data quantity on fisheries stock assessment. Aquatic Sciences 65:92–98.

Chernick, M. R., and R. A. LaBudde. 2011. An Introduction to Bootstrap Methods with Applications to R, 1st edition. Wiley Publishing.

Ciannelli, L., P. Fauchald, K. S. Chan, V. N. Agostini, and G. E. Dingsør. 2008. Spatial fisheries ecology : Recent progress and future prospects. Journal of Marine Systems 71:223–236.

Ciannelli, L., J. A. D. Fisher, M. Skern-mauritzen, M. E. Hunsicker, M. Hidalgo, K. T. Frank, and K. M. Bailey. 2013. Theory, consequences and evidence of eroding population spatial structure in harvested marine fishes : a review. Marine Ecology Progress Series 480:227–243.

Clark, W. G. 1999. Effects of an erroneous natural mortality rate on a simple age structured stock assessment. Canadian Journal of Fisheries and Aquatic Sciences 56(10):1721–1731.

Cochran, W. G. 1977. Sampling TechniquesThird. John Wiley & Sons, New York.

Cole, S. R., H. Chu, and S. Greenland. 2013. Maximum likelihood, profile likelihood, and penalized likelihood: A primer. Practice of Epidemiology 179(2):252–260.

Cope, J. M., and A. E. Punt. 2011. Reconciling stock assessment and management scales under conditions of spatially varying catch histories. Fisheries Research 107:22–38. Elsevier B.V.

Crone, P. R., and J. L. Valero. 2014. Evaluation of length- vs. age-composition data and associated selectivity assumptions used in stock assessments based on robustness of derived management quantities. Fisheries Research 158:165–171. Elsevier B.V.

Deriso, R. B. 1980. Harvesting strategies and parameter estimation for an age-structured model. Canadian Journal of Fisheries and Aquatic Sciences 37:268–282.

DFO. 2006. A Harvest Strategy Compliant with the Precautionary Approach.

DFO. 2009. Guidance for the Development of Rebuilding Plans under the Precautionary Approach Framework : Growing Stocks out of the Critical Zone Sustainable Fisheries Framework (SFF): A Fishery Decision-Making Framework Incorporating the Precautionary Approach. Ottawa.

DFO. 2012. Stock Assessment for the inside population of Yelloweye Rockfish (Sebastes ruberrimus) In British Columbia, Canada for 2010. DFO Can. Sci. Advis. Sec. Sci. Advis. Rep. 2011/084(April 2012):13.

DFO. 2017. Pacific Region Integrated Fisheries Management Plan: Groundfish.

Efron, B. 1979. Bootstrap methods: Another look at the jacknife. The Annals of Statistics 7(1):1–26.

Efron, B. 1985. Bootstrap confidence intervals for a class of parametric problems. Biometrika 72(1):45–58.

Forrest, R. E., M. K. Mcallister, M. W. Dorn, S. J. D. Martell, and R. D. Stanley. 2010. Hierarchical Bayesian estimation of recruitment parameters and reference points for Pacific rockfishes (Sebastes spp .) under alternative assumptions about the stock – recruit function. Canadian Journal of Fisheries and Aquatic Sciences 67:1611–1634.

Goethel, D. R., and A. M. Berger. 2017. Accounting for spatial complexities in the calculation of biological reference points : effects of misdiagnosing population structure. Canadian Journal of Fisheries and Aquatic Sciences 74:1878–1894.

Guan, W., J. Cao, Y. Chen, and M. Cieri. 2013. Impacts of population and fishery spatial structures on fishery stock assessment. Canadian Journal of Fisheries and Aquatic Sciences 70:1178–1189.

Haggarty, D. R., S. J. D. Martell, and J. B. Shurin. 2016. Lack of recreational fishing compliance may compromise effectiveness of Rockfish Conservation Areas in British Columbia. Canadian Journal of Fisheries and Aquatic Sciences 73(10):1587–1598.

Hilborn, R., and M. Mangel. 1997. The Ecological Detective. Confronting Models with Data. Princeton University Press, Princeton, New Jersey.

Hilborn, R., T. P. Quinn, D. E. Schindler, and D. E. Rogers. 2003. Biocomplexity and fisheries sustainability. Proceedings of the National Academy of Sciences of the United States of America 100(11):6564–6568.

Hilborn, R., and C. J. Walters. 1992. Quantitative Fisheries Stock Assessment: Choice, Dynamics, and Uncertainty. Routledge, Chapman, and Hall, New York.

Holland, D. S., and G. E. Herrera. 2010. Benefits and risks of increased spatial resolution in the management of fishery metapopulations under uncertainty. Natural Resource Modeling 23(4):494–520.

ICES. 2011. Report of the Workshop on the Implications of Stock Structure (WKISS). Copenhagen.

Jardim, E., M. Eero, A. Silva, C. Ulrich, L. Pawlowski, A. A. De Oliveira, I. Riveiro, S. J. Holmes, L. Ibaibarriaga, N. Alzorriz, L. Citores, F. Scott, A. Uriarte, P. Carrera, E. Duhamel, and I. Mosqueira. 2018. Testing spatial heterogeneity with stock assessment models. PLoS ONE 13(1).

Kerr, L. A., S. X. Cadrin, and A. I. Kovach. 2014. Consequences of a mismatch between biological and management units on our perception of Atlantic cod off New England. ICES Journal of Marine Science 71(6):1366–1381.

Love, M. S., M. Yoklavich, and L. Thorsteinson. 2002. Rockfishes of the Northeast Pacific. University of California Press, Berkeley.

Mace, P. M., and I. J. Doonan. 1988. A Generalised Bioeconomic Simulation Model for Fish Population Dynamics. New Zealand Fishery Assessment Research Document 88/4:53.

Mangel, M., J. Brodziak, and G. DiNardo. 2010. Reproductive ecology and scientific inference of steepness: a fundamental metric of population dynamics and strategic fisheries management. Fish and Fisheries 11:89–104.

Mangel, M., A. D. Maccall, J. Brodziak, E. J. Dick, R. E. Forrest, R. Pourzand, and S. Ralston. 2013a. A perspective on steepness , reference points , and stock assessment 940(April):930–940.

Mangel, M., A. D. MacCall, J. Brodziak, E. J. Dick, R. E. Forrest, R. Pourzand, and S. Ralston. 2013b. A perspective on steepness , reference points , and stock assessment. Canadian Journal of Fisheries and Aquatic Sciences 70:930–940.

Maunder, M. N., and K. R. Piner. 2015. Contemporary fisheries stock assessment: many issues still remain. ICES Journal of Marine Science 72(1):7–18.

Maunder, M. N., J. R. Sibert, A. Fonteneau, J. Hampton, P. Kleiber, and S. J. Harley. 2006. Interpreting catch per unit effort data to assess the status of individual stocks and communities. ICES Journal of Marine Science 63:1373–1385.

Meyer, R., and R. B. Millar. 1999. Bayesian stock assessment using a state – space implementation of the delay difference model. Canadian Journal of Fisheries and Aquatic Sciences 56:37–52.

Millar, R. B. 2002. Reference priors for Bayesian fisheries models. Canadian Journal of Fisheries and Aquatic Sciences 59:1492–1502.

Nelder, J. ., and R. Mead. 1965. A simplex algorithm for function minimization. Computer Journal 7:308–313.

Punt, A. E. 2019. Spatial stock assessment methods: A viewpoint on current issues and assumptions. Fisheries Research 213(January):132–143. Elsevier.

Punt, A. E., A. D. C. Smith, and M. T. Koopman. 2005. Using information for “data-rich” species to inform assessments of “data-poor” species through Bayesian stock assessment methods. Final report to Fisheries Research and Development Corporation Project No. 2002/094.

Punt, A. E., A. D. M. Smith, and G. Cui. 2002. Evaluation of management tools for Australia’s South East Fishery 2. How well can management quantities be estimated? Marine and Freshwater Research 53(3):631–644.

R Core Team. 2018. R: A language and environment for statistical computing. R Foundation for Statistical Computing, Vienna, Austria.

Ricker, W. E. 1975. Computation and Interpretation of Biological Statistics of Fish Populations. Page J. . Stevenson, J. Watson, R. H. Wigmore, and J. M. Reinhart, editorsBulletin 191. Department of the Environment Fisheries and Marine Service, Ottawa.

Schaefer, M. B. (n.d.). Fisheries dynamics and the concept of maximum equilibrium catch. Pages 53–63 Biological Session.

Schnute, J. 1985. A general theory for analysis of catch and effort data. Canadian Journal of Fisheries and Aquatic Sciences 42:414–429.

Siegle, M. R., E. B. Taylor, K. M. Miller, R. E. Withler, and K. L. Yamanaka. 2013. Subtle Population Genetic Structure in Yelloweye Rockfish (Sebastes ruberrimus) Is Consistent with a Major Oceanographic Division in British Columbia , Canada. PLoS ONE 8(8).

Starr, P. ., and R. Haigh. 2017. Stock assessment of the coastwide population of Shortspine Thornyhead (Sebastolobus alascanus) in 2015 off the British Columbia Coast.

Stephenson, R. L. 1999. Stock complexity in fisheries management : a perspective of emerging issues related to population sub-units. Fisheries Research 43:247–249.

Taylor, I. G., and C. Wetzel. 2011. Status of the US yelloweye rockfish resource in 2011 (Update of 2009 assessment model). Portland.

Thorson, J. T., M. W. Dorn, and O. S. Hamel. 2019. Steepness for west coast rockfishes: results from a twelve-year experiment in iterative regional meta-analysis. Fisheries Research 217:11–20.

Yamanaka, K. L., and A. R. Kronlund. 1997. Analysis of longline logbook data for the west coast Fisheries and Oceans Canada Stock Assessment Division Résum é. Canadian Stock Assessment Secretariat 134:1–42.

Yamanaka, K. L., L. C. Lacko, R. Withler, C. Grandin, J. K. Lochead, J. C. Martin, N. Olsen, S. S. Wallace, O. Canada, P. B. Station, and B. Creek. 2006. A review of yelloweye rockfish Sebastes ruberrimus along the Pacific coast of Canada: biology, distribution and abundance trends.

Yamanaka, K. L., and G. Logan. 2010. Developing British Columbia's inshore rockfish conservation strategy. Marine and Coastal Fisheries: Dynamics, Management, and Ecosystem Science 2(1):28–46.

Yamanaka, K. L., M. McAllister, M. . Etienne, A. Edwards, and Haigh R. 2018. Stock Assessment for the outside population of Yelloweye Rockfish (Sebastes ruberrimus) In British Columbia, Canada for 2014. Can. Sci. Advis. Sec. Sci. Advis. Rep.

Yamanaka, K. L., R. E. Withler, and K. M. Miller. 2000. Structure of yelloweye rockfish (Sebastes ruberrimus) populations in British Columbia. Canadian Stock Assessment Secretariat 2000/172:1–32.

Appendix A: Growth Analyses

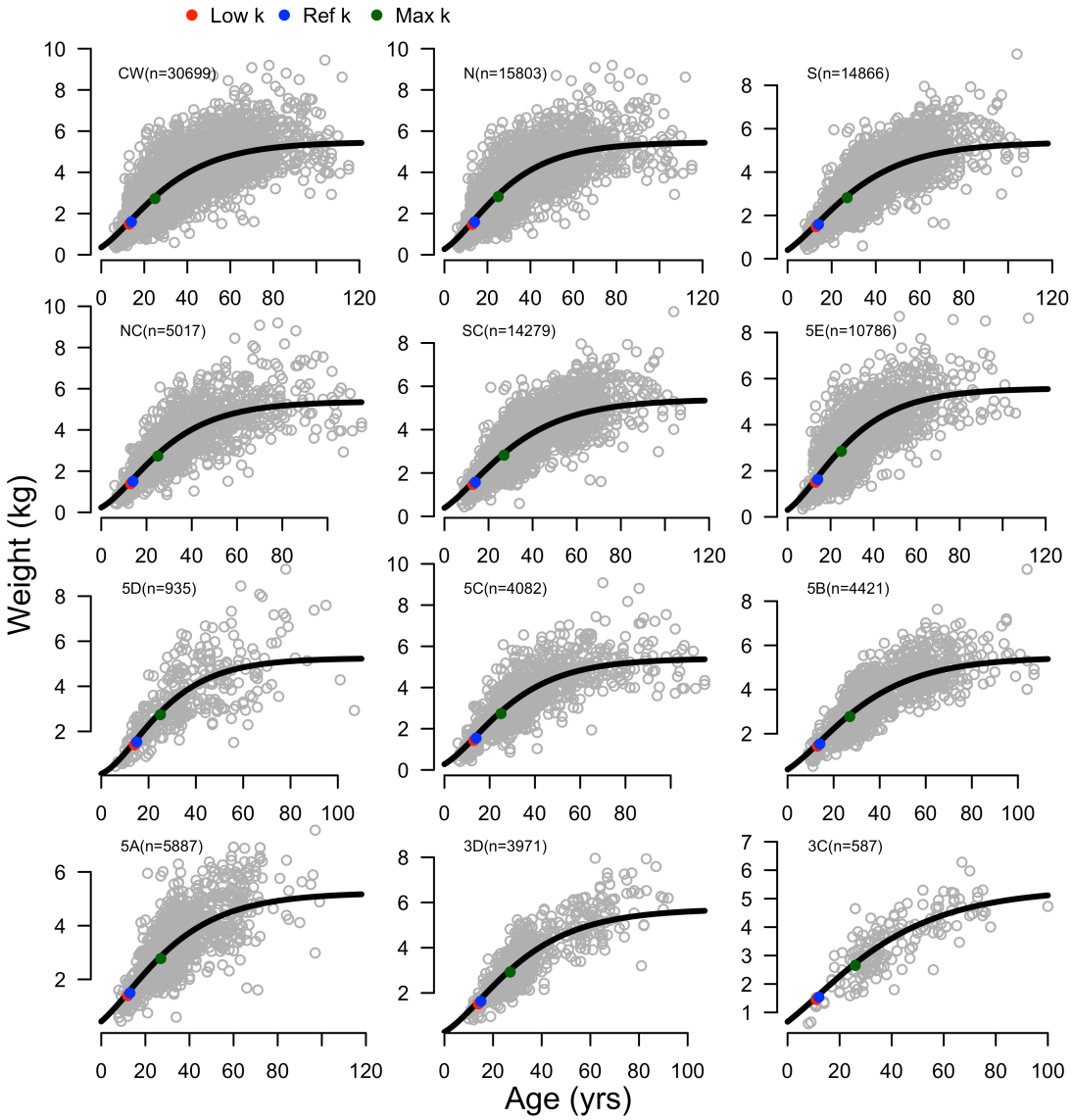

Figure A1. Estimated weight-at-age from the growth analyses on Yelloweye stocks. Data for females and males are combined. Ages used to parameterize various model runs are indicated by coloured points. Total numbers of individuals included in the analysis are shown on each panel. Note the low number of biological samples collected from Areas 5D and 3C.

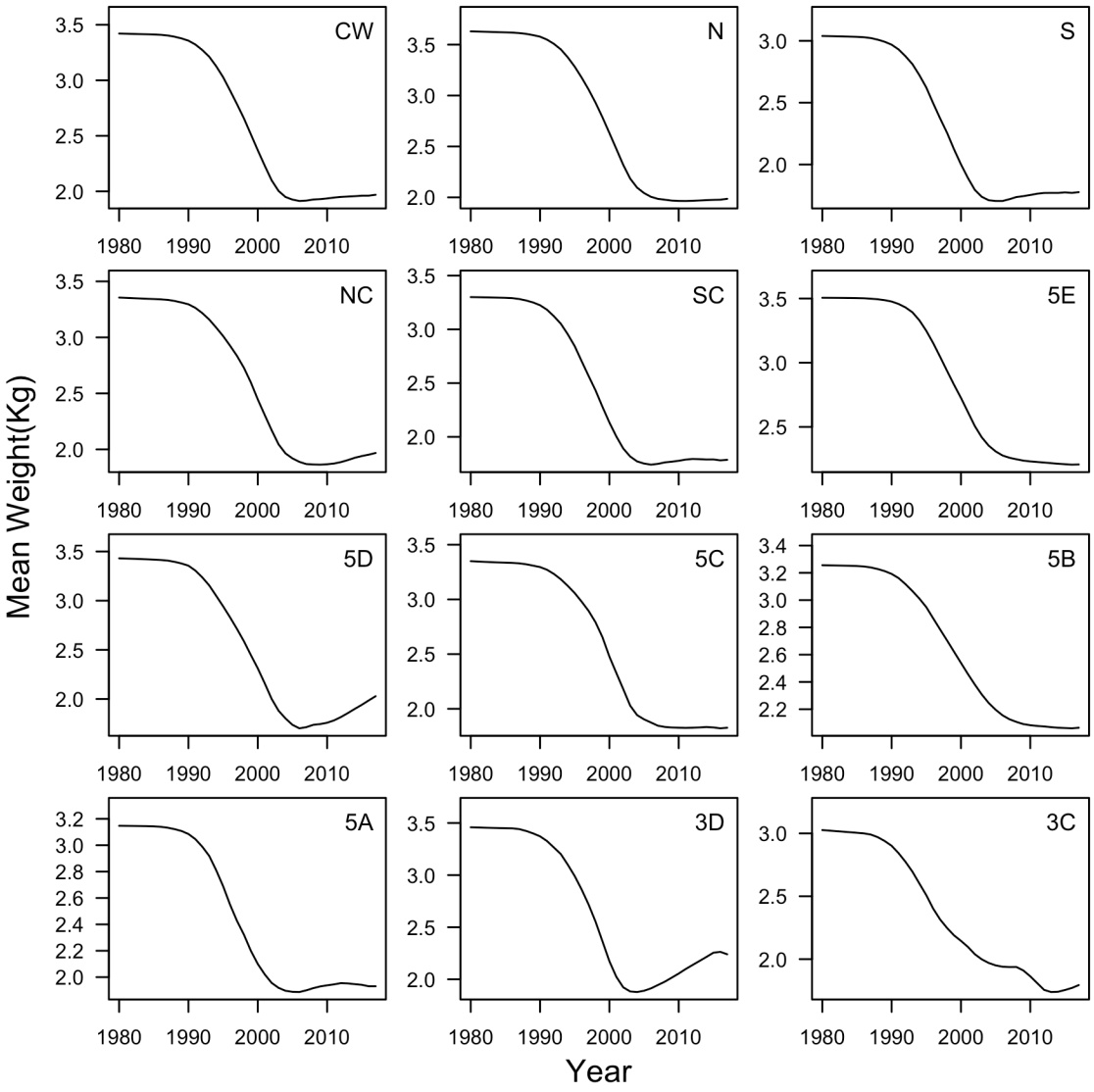

Figure A2. Change in mean weight over time, from reference case runs of the delay-difference stock assessment model for each Yelloweye stock showing a consistent declining trend in mean weight in the 1990s.

Table A1. von-Bertalanffy growth parameters for the spatially disaggregated Yelloweye stocks, where *K* is the growth rate coefficient, t_0 is the age at which the average size is zero, and L_{inf} is the average length at maximum age. Parameters were used to estimate length-at-age, $L_t = L_\infty(1-e^{-K(t-t_0)})$. These values were used to examine differences between spatial scales, but were not used to parameterize delay-difference models.

Stock	L_{inf} (cm)	*K*	t_0
CW	65.9	0.044	8.42E-06
N	65.9	0.049	6.38E-05
S	65.6	0.042	2.56E-06
NC	65.3	0.049	1.04E-04
SC	65.7	0.042	3.27E-06
5E	66.6	0.047	4.38E-05
5D	64.8	0.055	1.78E-03
5C	65.5	0.047	4.01E-05
5B	65.7	0.041	2.74E-06
5A	65.3	0.042	1.28E-06
3D	67.1	0.044	4.86E-05
3C	64.6	0.035	1.92E-09

Von-Bertalanffy parameters were very similar between spatial scales, with the exception of Areas 5D and 3C, which is likely a result of low sampling rates in these two areas.

Appendix B: Results of Sensitivity Analyses

Table B1. Median estimates for key parameters from model runs fit to individual survey abundance indices.

	All surveys			IPHC			PHMA		
Stock ID	**B_0**	***h***	**B_{2017}/B_0**	**B_0**	***h***	**B_{2017}/B_0**	**B_0**	***h***	**B_{2017}/B_0**
CW_N	15023	0.863	0.044	15133	0.824	0.045	16080	0.787	0.125
CW_S	15023	0.863	0.044	15133	0.824	0.045	15213	0.804	0.049
N	7031	0.885	0.061	7042	0.820	0.049	7545	0.777	0.137
S	8128	0.868	0.036	8161	0.841	0.034	8136	0.872	0.039
NC	3936	0.684	0.047	4029	0.513	0.044	3759	0.942	0.021
SC	7480	0.898	0.042	7519	0.875	0.045	7535	0.872	0.048
5E	3239	0.882	0.118	3199	0.900	0.105	3528	0.755	0.192
5D	1460	0.536	0.031	1460	0.536	0.031	1460	0.536	0.031
5C	2410	0.875	0.046	2469	0.690	0.044	2622	0.801	0.146
5B	2798	0.787	0.109	2802	0.775	0.108	2883	0.772	0.141
5A	2998	0.731	0.064	2933	0.758	0.033	2971	0.842	0.083
3D	2076	0.530	0.023	2061	0.556	0.018	2085	0.641	0.061
3C	924	0.559	0.032	912	0.620	0.033	906	0.608	0.015

Table B2. Successful (nS) versus total bootstrap (nB) iterations for sensitivity test model runs for each stock.

Stock	low_*h*_ nS	low_*h*_ nB	high_*h*_n S	high_*h*_n B	low_*M*_n S	low_*M*_n B	high_*M*_ nS	high_*M*_ nB	low_*k*_ nS	low_*k*_ nB	high_*k*_n S	high_*k* _nB
CW	1000	1000	1000	1000	1000	1000	1000	1001	1000	1000	1000	1000
N	1000	1000	1000	1000	1000	1000	2000	2001	1000	1000	1000	1000
S	2000	2000	2000	2001	1000	1000	2000	2007	1000	1000	1000	1000
NC	1000	1000	1000	1000	1000	1000	2000	2000	1000	1000	1000	1000
SC	1000	1000	1000	1000	1000	1000	5000	5000	1000	1000	1000	1000
5E	1000	1000	1000	1000	1000	1000	1000	1000	1000	1000	1000	1001
5D	2000	2617	2000	2300	2000	2016	2000	2640	2000	2320	1000	1001
5C	1000	1000	1000	1000	1000	1000	2000	2003	1000	1000	1000	1000
5B	1000	1000	1000	1000	1000	1000	1000	1000	1000	1000	1000	1000
5A	2000	2000	5000	5002	1000	1000	2000	2006	1000	1003	2000	2000
3D	3000	3000	2000	2073	5000	5116	5000	5003	2000	2071	1000	1000
3C	1000	1100	2000	2235	1000	1002	1000	1198	1000	1092	1000	1004

Table B3. Median estimates for parameters, reference points, and derived quantities from model runs parameterized with a low standard deviation on the penalty for steepness.

Stock ID	*h*	B_0	*MSY*	B_{MSY}	F_{MSY}	B_{2017}/B_0	F_{2017}/F_{MSY}
Scenario One							
CW	0.743 *(0.61, 0.86)*	15489 *(14991, 16191)*	214 *(182, 243)*	4171 *(3269, 5122)*	0.054 *(0.037, 0.078)*	0.061 *(0.037, 0.101)*	2.54 *(1.64, 3.62)*
Scenario Two							
N	0.712 *(0.61, 0.81)*	7336 *(7106, 7831)*	93 *(81, 103)*	2110 *(1788, 2414)*	0.046 *(0.035, 0.06)*	0.087 *(0.052, 0.161)*	2.21 *(1.15, 3.78)*
S	0.746 *(0.61, 0.87)*	8375 *(8188, 8759)*	119 *(101, 137)*	2234 *(1737, 2786)*	0.056 *(0.038, 0.083)*	0.051 *(0.03, 0.091)*	2.6 *(1.67, 3.85)*
Scenario Three							
NC	0.687 *(0.57, 0.80)*	3934 *(3846, 4083)*	49 *(42, 56)*	1161 *(984, 1361)*	0.044 *(0.032, 0.059)*	0.046 *(0.025, 0.092)*	4.06 *(1.93, 7.07)*
SC	0.727 *(0.60, 0.85)*	7816 *(7556, 8231)*	103 *(87, 118)*	2184 *(1731, 2679)*	0.049 *(0.035, 0.071)*	0.069 *(0.042, 0.12)*	2.13 *(1.29, 3.08)*
5E	0.699 *(0.65, 0.75)*	3494 *(3254, 4690)*	45 *(40, 61)*	1020 *(910, 1364)*	0.046 *(0.04, 0.053)*	0.173 *(0.09, 0.412)*	1.2 *(0.37, 2.53)*
3C	0.67 *(0.57,0.77)*	902 *(884, 923)*	11 *(10, 12)*	266 *(227, 304)*	0.043 *(0.033, 0.057)*	0.031 *(0.021, 0.057)*	4.66 *(2.38, 8.5)*
Scenario Four							
5D	0.647 *(0.54, 0.73)*	1452 *(1437, 3276)*	17 *(14, 41)*	466 *(403, 982)*	0.04 *(0.029, 0.05)*	0.045 *(0.013, 0.646)*	4.06 *(0.12, 18.5)*
5C	0.699 *(0.61, 0.79)*	2496 *(2433, 2618)*	32 *(28, 35)*	725 *(626, 820)*	0.046 *(0.035, 0.059)*	0.061 *(0.035, 0.12)*	3.07 *(1.5, 5.31)*
5B	0.696 *(0.63, 0.78)*	2870 *(2741, 3205)*	36 *(32, 41)*	836 *(719, 955)*	0.045 *(0.037, 0.057)*	0.12 *(0.07, 0.234)*	1.34 *(0.61, 2.36)*
5A	0.691 *(0.62,0.77)*	3028 *(2947, 3173)*	38 *(34, 42)*	883 *(769, 988)*	0.045 *(0.037, 0.056)*	0.068 *(0.039, 0.13)*	1.62 *(0.84, 2.77)*
3D	0.621 *(0.51, 0.72)*	2046 *(2017, 2108)*	23 *(19, 27)*	649 *(569, 754)*	0.037 *(0.027, 0.048)*	0.02 *(0.011, 0.063)*	13.63 *(4.07, 27.4)*

Table B4. Median estimates for parameters, reference points, and derived quantities from model runs parameterized with a high standard deviation on the penalized log-likelihood for steepness.

Stock ID	*h*	B_0	*MSY*	B_{MSY}	F_{MSY}	B_{2017}/B_0	F_{2017}/F_{MSY}
Scenario One							
CW	0.873 *(0.678, 0.935)*	14984 *(14733, 15760)*	244 *(199, 261)*	3211 *(2625, 4608)*	0.081 *(0.045, 0.106)*	0.043 *(0.027, 0.08)*	2.52 *(1.7, 3.6)*
Scenario Two							
N	0.914 *(0.683, 0.986)*	6989 *(6848, 7406)*	113 *(92, 122)*	1421 *(1061, 2155)*	0.084 *(0.043, 0.126)*	0.059 *(0.037, 0.107)*	1.93 *(1.1, 3.2)*
S	0.877 *(0.661, 0.934)*	8113 *(7986, 8585)*	137 *(108, 145)*	1706 *(1431, 2541)*	0.085 *(0.044, 0.11)*	0.035 *(0.021, 0.071)*	2.65 *(1.7, 3.8)*
Scenario Three							
NC	0.722 *(0.426, 0.869)*	3910 *(3813, 4195)*	51 *(30, 60)*	1108 *(866, 1624)*	0.048 *(0.019, 0.074)*	0.044 *(0.023, 0.092)*	3.95 *(2.0, 7.6)*
SC	0.727 *(0.598, 0.853)*	7816 *(7556, 8231)*	103 *(87, 118)*	2184 *(1731, 2679)*	0.049 *(0.035, 0.071)*	0.069 *(0.042, 0.12)*	2.13 *(1.3, 3.1)*
5E	0.933 *(0.67, 0.99)*	3197 *(3059, 3715)*	55 *(42, 61)*	603 *(445, 1072)*	0.097 *(0.042, 0.14)*	0.106 *(0.058, 0.256)*	1.04 *(0.44, 2.2)*
3C	0.638 *(0.362, 0.826)*	907 *(875, 981)*	10 *(5, 13)*	278 *(204, 407)*	0.039 *(0.014, 0.068)*	0.031 (0.019, 0.058)	5.25 *(2.3, 15.3)*
Scenario Four							
5D	0.622 *(0.43, 0.796)*	1469 *(1438, 3731)*	17 *(11, 53)*	509 *(404, 995)*	0.037 *(0.02, 0.06)*	0.049 *(0.011, 0.696)*	4.4 *(0.07, 25.4)*
5C	0.926 *(0.725, 0.989)*	2388 *(2351, 2501)*	40 *(33, 43)*	462 *(340, 699)*	0.093 *(0.049, 0.139)*	0.042 *(0.025, 0.079)*	2.31 *(1.2, 4.0)*
5B	0.846 *(0.556, 0.978)*	2763 *(2641, 3099)*	42 *(30, 49)*	636 *(399, 1034)*	0.07 *(0.03, 0.131)*	0.102 *(0.06, 0.198)*	1.07 *(0.48,2.3)*
5A	0.931 *(0.565, 0.985)*	2855 *(2801, 3178)*	49 *(32, 52)*	530 *(395, 1061)*	0.098 *(0.032, 0.143)*	0.043 *(0.026,0.112)*	1.3 *(0.79, 2.1)*
3D	0.545 *(0.342, 0.75)*	2074 *(2018, 2283)*	20 *(11, 28)*	717 *(570, 1011)*	0.03 *(0.012, 0.053)*	0.023 *(0.01, 0.145)*	14.94 *(2.1, 36.4)*

Table B5. Median estimates for parameters, reference points, and derived quantities from model runs parameterized with a low fixed natural mortality rate.

Stock ID	*h*	B_0	*MSY*	B_{MSY}	F_{MSY}	B_{2017}/B_0	F_{2017}/F_{MSY}
Scenario One							
CW	0.769 *(0.59, 0.9)*	19286 *(18631, 20496)*	148 *(117, 169)*	5182 *(4073, 6639)*	0.029 *(0.018, 0.042)*	0.095 *(0.063, 0.151)*	2.4 *(1.35, 4.0)*
Scenario Two							
N	0.764 *(0.61, 0.86)*	9090 *(8621, 10337)*	67 *(53, 77)*	2523 *(2116, 3161)*	0.027 *(0.018, 0.035)*	0.127 *(0.075, 0.241)*	2.08 *(0.97, 4.2)*
S	0.77 *(0.61, 0.9)*	10355 *(10032, 10887)*	82 *(66, 94)*	2737 *(2123, 3423)*	0.031 *(0.02, 0.045)*	0.075 *(0.049, 0.121)*	2.63 *(1.5, 4.4)*
Scenario Three							
NC	0.753 *(0.57, 0.89)*	4711 *(4591, 4947)*	35 *(27, 41)*	1311 *(1050, 1649)*	0.027 *(0.017, 0.04)*	0.06 *(0.036, 0.11)*	4.06 *(2.1, 7.9)*
SC	0.761 *(0.59, 0.87)*	9630 *(9290, 10369)*	71 *(57, 81)*	2642 *(2224, 3299)*	0.028 *(0.018, 0.037)*	0.097 *(0.062, 0.173)*	2.21 *(1.1, 3.7)*
5E	0.76 *(0.66, 0.82)*	4511 *(3972, 7031)*	34 *(27, 53)*	1255 *(1060, 1931)*	0.028 *(0.022, 0.032)*	0.232 *(0.115, 0.516)*	1.13 *(0.33, 2.9)*
3C	0.734 *(0.55, 0.92)*	1081 *(1054, 1113)*	8 *(6, 9)*	304 *(219, 381)*	0.026 *(0.016, 0.043)*	0.026 *(0.015, 0.054)*	7.84 *(3.46, 18.0)*
Scenario Four							
5D	0.747 *(0.56, 0.92)*	1697 *(1651, 2145)*	13 *(10, 16)*	481 *(352, 628)*	0.028 *(0.017, 0.045)*	0.041 *(0.011, 0.278)*	5.53 *(0.65, 22.2)*
5C	0.757 *(0.61, 0.86)*	3021 *(2927, 3228)*	23 *(19, 25)*	832 *(706, 1007)*	0.028 *(0.019, 0.036)*	0.078 *(0.046, 0.146)*	3.31 *(1.6, 6)*
5B	0.753 *(0.65, 0.83)*	3698 *(3403, 4762)*	27 *(22, 35)*	1035 *(875, 1323)*	0.027 *(0.021, 0.033)*	0.177 *(0.098, 0.373)*	1.19 *(0.42, 2.5)*
5A	0.753 *(0.65, 0.86)*	3583 *(3482, 3822)*	26 *(23, 29)*	989 *(843, 1146)*	0.027 *(0.021, 0.036)*	0.07 *(0.04, 0.139)*	2.22 *(1.1, 4.0)*
3D	0.757 *(0.51, 0.88)*	2416 *(2378, 2504)*	18 *(12, 20)*	664 *(548, 895)*	0.028 *(0.014, 0.038)*	0.021 *(0.01, 0.052)*	15.32 *(6, 33.2)*

Table B6. Median estimates for parameters, reference points, and derived quantities from model runs parameterized with a high fixed natural mortality rate.

Stock ID	*h*	B_0	*MSY*	B_{MSY}	F_{MSY}	B_{2017}/B_0	F_{2017}/F_{MSY}
Scenario One							
CW	0.748 *(0.539, 0.847)*	14394 *(14005, 15483)*	239 *(181, 265)*	3807 *(3111, 5298)*	0.066 *(0.036, 0.091)*	0.056 *(0.032, 0.113)*	2.44 *(1.5, 3.7)*
Scenario Two							
N	0.828 *(0.642, 0.915)*	6617 *(6463, 7020)*	116 *(95, 126)*	1587 *(1280, 2164)*	0.077 *(0.046, 0.106)*	0.059 *(0.033, 0.114)*	2.2 *(1.3, 3.6)*
S	0.726 *(0.506, 0.836)*	7850 *(7627, 8563)*	130 *(95, 147)*	2133 *(1718, 3092)*	0.064 *(0.033, 0.091)*	0.053 *(0.03, 0.116)*	2.39 *(1.5, 3.7)*
Scenario Three							
NC	0.595 *(0.424, 0.746)*	3753 *(3632, 12049)*	48 *(33, 174)*	1239 *(988, 3596)*	0.041 *(0.023, 0.062)*	0.046 *(0.023, 0.757)*	4.68 *(0.07, 9.1)*
SC	0.78 *(0.551, 0.881)*	7182 *(6991, 7737)*	121 *(91, 134)*	1835 *(1474, 2625)*	0.07 *(0.036, 0.097)*	0.056 *(0.033, 0.112)*	2.04 *(1.3, 3.0)*
5E	0.867 *(0.655, 0.971)*	2966 *(2842, 3451)*	56 *(46, 63)*	649 *(437, 1020)*	0.092 *(0.049, 0.155)*	0.093 *(0.05, 0.237)*	1.29 *(0.56, 2.4)*
3C	0.612 *(0.425, 0.764)*	852 *(825, 902)*	11 *(8, 14)*	268 *(211, 348)*	0.044 *(0.023, 0.069)*	0.034 *(0.021, 0.059)*	4.54 *(2.18, 10.44)*
Scenario Four							
5D	0.676 *(0.456, 0.713)*	1440 *(1368, 3696)*	21 *(13, 56)*	519 *(412, 1062)*	0.052 *(0.026, 0.057)*	0.133 *(0.014, 0.722)*	1.21 *(0.07, 18.7)*
5C	0.745 *(0.515, 0.888)*	2311 *(2233, 2515)*	37 *(27, 43)*	626 *(470, 879)*	0.063 *(0.032, 0.099)*	0.058 *(0.028, 0.131)*	2.61 *(1.2, 4.9)*
5B	0.772 *(0.565, 0.922)*	2569 *(2460, 2813)*	43 *(34, 50)*	662 *(458, 926)*	0.068 *(0.038, 0.118)*	0.092 *(0.053, 0.176)*	1.29 *(0.65, 2.3)*
5A	0.669 *(0.439, 0.881)*	2866 *(2712, 3125)*	41 *(27, 52)*	851 *(565, 1173)*	0.051 *(0.024, 0.099)*	0.073 *(0.038, 0.151)*	1.41 *(0.73, 2.62)*
3D	0.476 *(0.341, 0.686)*	1985 *(1931, 5013)*	20 *(12, 73)*	740 *(625, 1463)*	0.028 *(0.015, 0.053)*	0.032 *(0.013, 0.701)*	12.29 *(0.11, 34.3)*

Table B7. Median estimates for parameters, reference points, and derived quantities from model runs parameterized with a low age at knife-edge recruitment.

Stock ID	*h*	B_0	*MSY*	B_{MSY}	F_{MSY}	B_{2017}/B_0	F_{2017}/F_{MSY}
Scenario One							
CW	0.877 *(0.661, 0.949)*	15231 *(14918, 16190)*	245 *(194, 262)*	3280 *(2597, 4873)*	0.079 *(0.042, 0.109)*	0.047 *(0.03, 0.089)*	2.28 *(1.58, 3.2)*
Scenario Two							
N	0.863 (*0.629, 0.958)*	7107 *(6908, 7609)*	109 *(86, 120)*	1631 *(1233, 2386)*	0.071 *(0.037, 0.104)*	0.07 *(0.041, 0.126)*	1.9 *(1.11, 3.09)*
S	0.913 *(0.671, 0.961)*	8347 *(8222, 8905)*	137 *(108, 144)*	1664 *(1377, 2673)*	0.088 *(0.042, 0.113)*	0.036 *(0.025, 0.072)*	2.36 *(1.72, 3.26)*
Scenario Three							
NC	0.725 *(0.492, 0.878)*	3977 *(3863, 4222)*	51 *(36, 60)*	1131 *(873, 1531)*	0.047 *(0.024, 0.073)*	0.046 *(0.024, 0.092)*	3.82 *(1.99, 6.66)*
SC	0.938 *(0.658, 0.984)*	7526 *(7410, 8178)*	126 *(96, 131)*	1421 *(1141, 2500)*	0.095 *(0.04, 0.125)*	0.041 *(0.028, 0.091)*	1.98 *(1.43, 2.67)*
5E	0.799 *(0.628, 0.93)*	3434 *(3198, 4322)*	49 *(40, 61)*	886 *(635, 1213)*	0.059 *(0.037, 0.091)*	0.15 *(0.079, 0.358)*	1.11 *(0.39, 2.31)*
3C	0.683 *(0.481, 0.843)*	930 *(904, 973)*	11 *(8, 13)*	277 *(216, 356)*	0.042 *(0.023, 0.065)*	0.029 *(0.018, 0.054)*	4.95 *(2.27, 11.89)*
Scenario Four							
5D	0.664 *(0.494, 0.784)*	1476 *(1453, 3382)*	18 *(13, 42)*	468 *(389, 1005)*	0.041 *(0.025, 0.056)*	0.035 *(0.01, 0.652)*	5.33 *(0.11, 20.88)*
5C	0.84 *(0.605,0.96)*	2473 *(2405, 2627)*	37 *(28, 41)*	591 *(427, 845)*	0.065 *(0.034, 0.104)*	0.052 *(0.028, 0.099)*	2.56 *(1.36, 4.34)*
5B	0.776 *(0.585, 0.93)*	2862 *(2708,3192)*	40 *(31, 46)*	752 *(519, 1020)*	0.055 *(0.033, 0.092)*	0.115 *(0.065, 0.222)*	1.16 *(0.54, 2.12)*
5A	0.746 *(0.541, 0.954)*	3035 *(2871,3252)*	40 *(31, 49)*	829 *(506, 1118)*	0.051 *(0.029, 0.105)*	0.061 *(0.03, 0.122)*	1.55 *(0.85, 2.7)*
3D	0.63 *(0.426,0.776)*	2082 *(2037,2196)*	23 *(15, 28)*	658 *(536, 868)*	0.037 *(0.019, 0.055)*	0.023 *(0.011, 0.068)*	11.98 *(4.05, 25.07)*

Table B8. Median estimates for parameters, reference points, and derived quantities from model runs parameterized with the max age at knife-edge recruitment.

Stock ID	*h*	B_0	*MSY*	B_{MSY}	F_{MSY}	B_{2017}/B_0	F_{2017}/F_{MSY}
Scenario One							
CW	0.738 *(0.703, 0.764)*	25445 *(15968, 53848)*	410 *(252, 860)*	6446 *(4049, 13724)*	0.067 *(0.06, 0.073)*	0.55 *(0.264, 0.79)*	0.14 *(0.05, 0.48)*
Scenario Two							
N	0.739 *(0.71, 0.762)*	10322 *(7027, 22373)*	167 *(111, 360)*	2622 *(1777, 5730)*	0.067 *(0.061, 0.072)*	0.492 *(0.234, 0.769)*	0.19 *(0.06, 0.63)*
S	0.74 *(0.73, 0.754)*	12362 *(8418, 24636)*	201 *(138, 400)*	3102 *(2106, 6208)*	0.068 *(0.066, 0.072)*	0.499 *(0.245, 0.752)*	0.15 *(0.05, 0.44)*
Scenario Three							
NC	0.738 *(0.711, 0.766)*	5694 *(3936, 12086)*	91 *(63, 192)*	1459 *(995, 3104)*	0.066 *(0.061, 0.072)*	0.496 *(0.251, 0.766)*	0.17 *(0.05, 0.49)*
SC	0.836 *(0.822, 0.852)*	12146 *(7784, 25866)*	227 *(147, 482)*	2511 *(1600, 5372)*	0.096 *(0.091, 0.103)*	0.544 *(0.269, 0.788)*	0.09 *(0.03, 0.27)*
5E	0.744 *(0.641, 0.796)*	2952 *(2759, 4524)*	48 *(39, 72)*	760 *(644, 1196)*	0.068 *(0.049, 0.081)*	0.163 *(0.089, 0.472)*	1.03 *(0.24, 2.25)*
3C	0.738 *(0.723, 0.756)*	1014 *(804, 1669)*	16 *(13, 27)*	253 *(198, 420)*	0.068 *(0.064, 0.072)*	0.371 *(0.18, 0.626)*	0.23 (*0.08, 0.61)*
Scenario Four							
5D	0.74 *(0.723, 0.76)*	1815 *(1381, 3493)*	29 *(22, 56)*	462 *(349, 894)*	0.067 *(0.064, 0.071)*	0.438 *(0.233, 0.715)*	0.2 *(0.06, 0.5)*
5C	0.739 (*0.701, 0.773)*	3298 *(2340, 6596)*	53 *(37, 105)*	838 *(587, 1690)*	0.066 *(0.059, 0.074)*	0.436 *(0.181, 0.723)*	0.22 *(0.07,0.74)*
5B	0.742 *(0.669, 0.784)*	2541 *(2365, 3871)*	42 *(35, 62)*	646 *(564, 988)*	0.068 *(0.054, 0.078)*	0.178 *(0.104, 0.476)*	0.69 *(0.17, 1.37)*
5A	0.741 *(0.732, 0.755)*	4057 *(2798, 7976)*	67 *946, 131)*	1013 *(692, 2009)*	0.069 (0.067, 0.072)	0.48 *(0.223, 0.739)*	0.11 *(0.04, 0.35)*
3D	0.742 *(0.736,0.752)*	2874 *92031, 5429)*	46 *(33, 88)*	726 *(509, 1364)*	0.068 *(0.066, 0.07)*	0.494 *(0.264, 0.736)*	0.21 *(0.08, 0.55)*

Appendix C: Average Recruitment Relationship Results

Initial attempts to fit the average recruitment SRR models yielded poor results. There were large differences between the MLE and median bootstrap estimates, and fits to the survey indices were very poor, similar to the fits for 5D and 3C in the plot above (figure C1). To check if *optim* was finding false minima, I used a grid search to estimate a range for the upper and lower values to parameterize the search interval for *optim.* I did this by examining the likelihood profile over each interval and progressively narrowing the search window. When an acceptable likelihood profile was found (if one could be found) that search interval was then used to parameterize the *optim* optimization procedure i.e. this procedure provided the upper and lower values for the *optim* search. This lead to improved fits for most stocks, although 5D and 3C remain problematic, most likely due to data scarcity.

Initial biomass estimates are similar to the Beverton-Holt reference case runs at coarser spatial scales, but there are more differences at the PGMA level. Several of the biomass time series indicate increasing biomass near the end of the time series i.e. CW, S, and NC.

Plots showing the sum of component stock biomass compared to aggregate stock biomass are shown in figure C3. These results for the average recruitment SRR are very similar to the results from the Beverton-Holt SRR.

Stock status for the average recruitment SRR was much more optimistic for most stocks than for the Beverton-Holt SRR (figure C2), except NC, which is slightly better, but still in the critical zone.

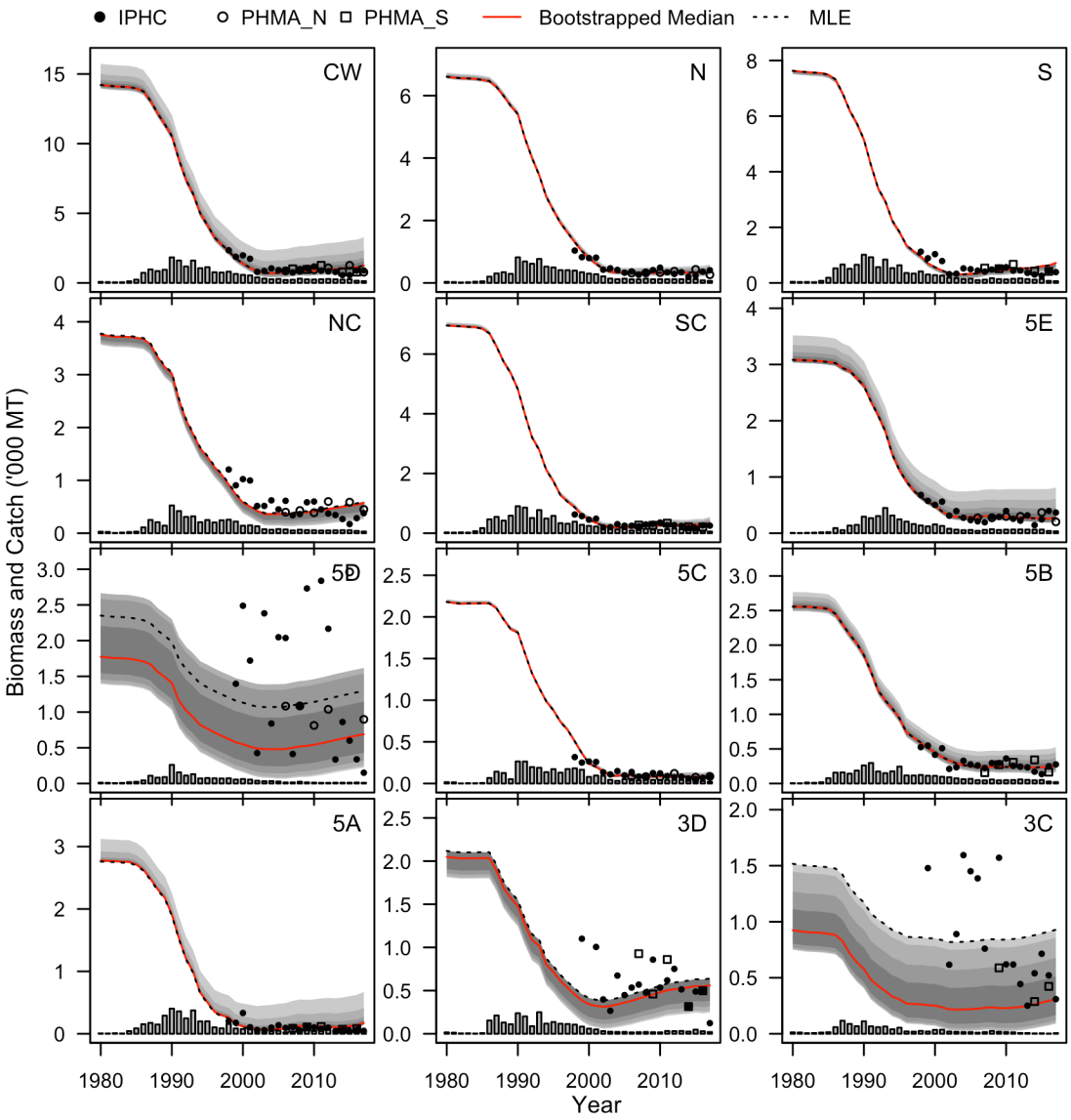

Figure C1. Estimated biomass time series for the average recruitment SRR. Both the MLE and median bootstrap estimated time series are plotted. Catch is shown as vertical bars on the x-axis, and annual survey CPUEs are plotted as points. 50%, 75%, 90% and 95% bootstrapped confidence intervals are shown as polygons in ascending shades of grey. The time series are truncated, as there was relatively little change in biomass prior to the mid 80s.

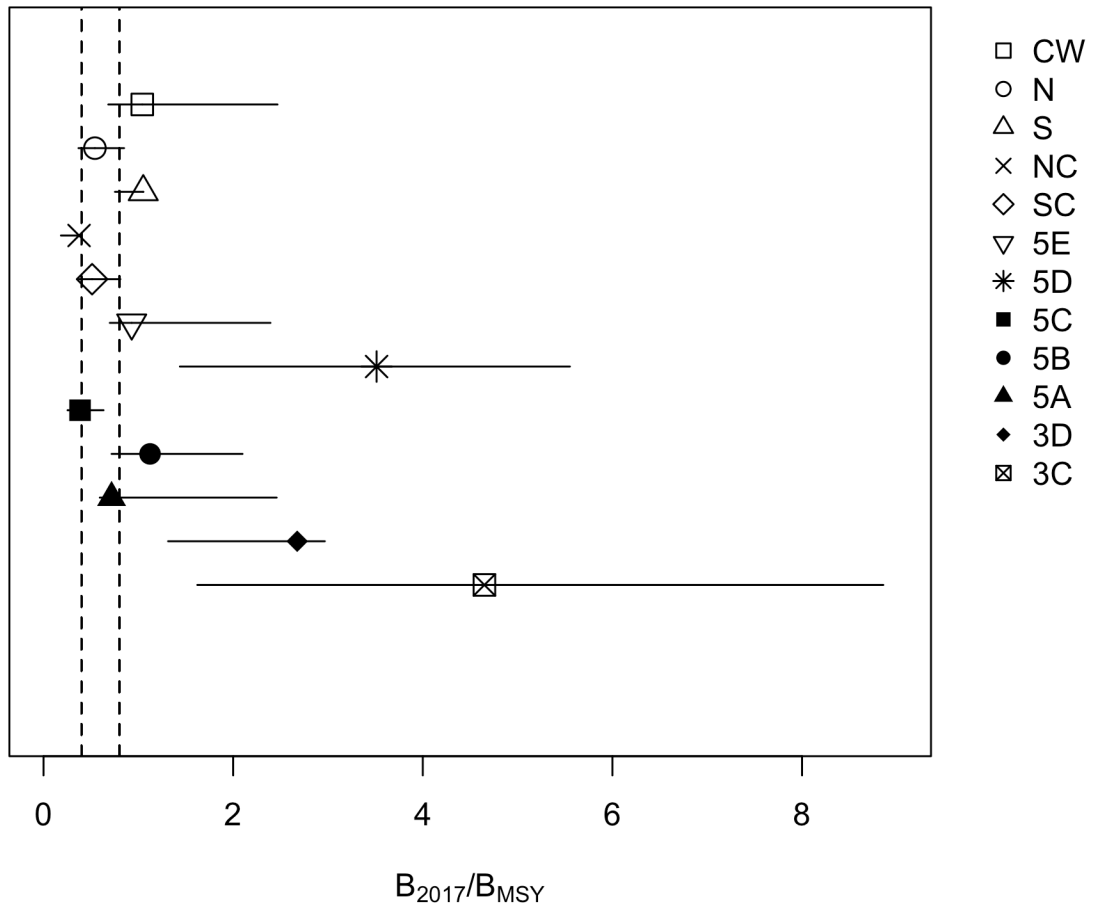

Figure C2. Estimated stock status in 2017 for the average recruitment SRR. Yelloweye stocks are arranged generally in order of the spatial scenarios e.g. the first scenario, the coast-wide stock is plotted first. Horizontal lines indicate 95% bootstrapped confidence intervals. Dashed vertical lines demarcate the critical, cautious, and healthy status zones.

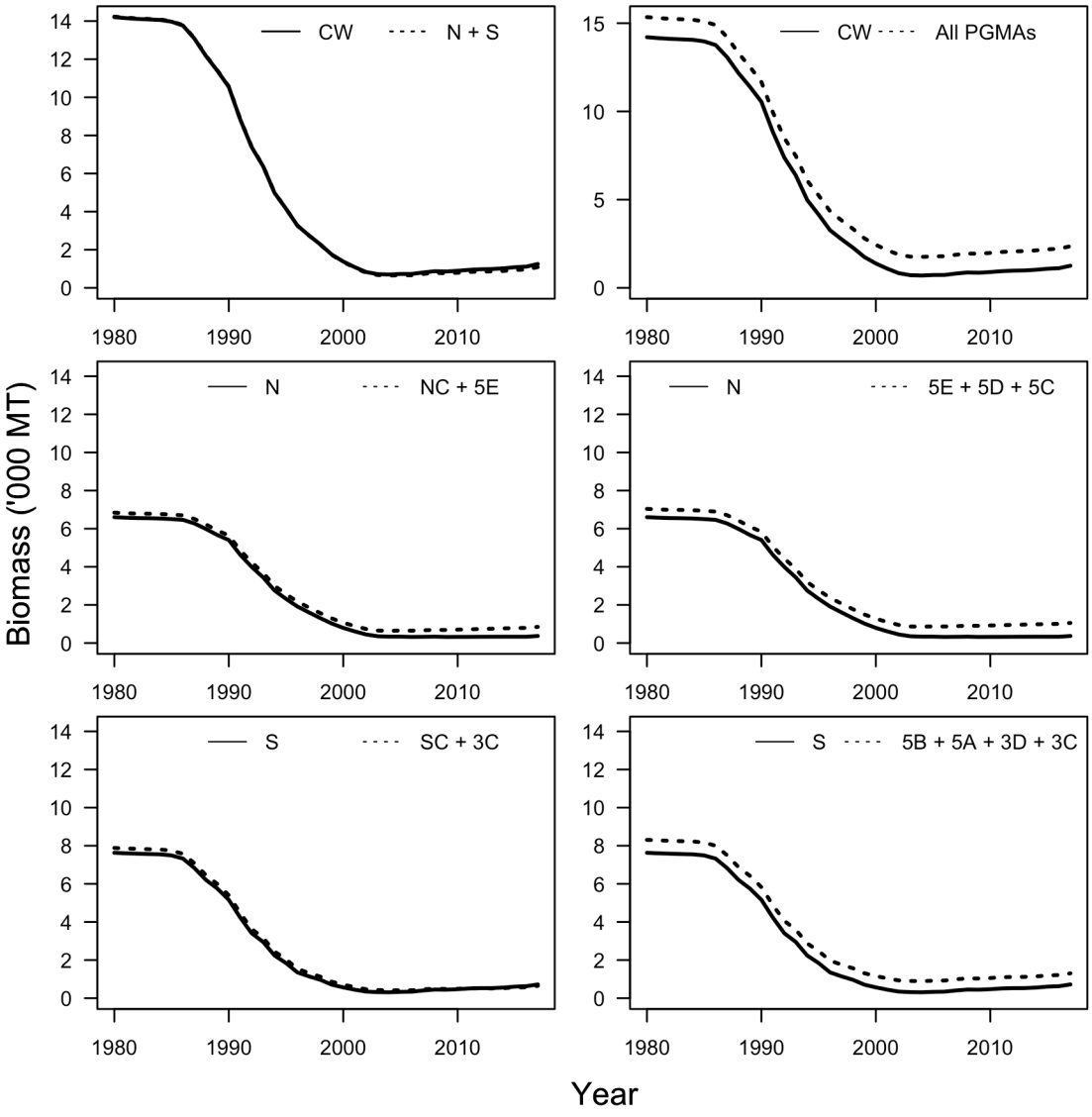

Figure C3. Median estimated biomass time series for each aggregate stock and the summed estimated biomass of its components stocks for the average recruitment SRR. Refer to figure 1 for the map showing spatial breakdown of aggregate stocks into component stocks. Time series have been truncated.